Chem. Rev. **2001,** *101,* 1267−1300 **1267**

Big Is Beautiful−“Aromaticity” Revisited from the Viewpoint of Macromolecular and Supramolecular Benzene Chemistry

Mark D. Watson, Andreas Fechtenkötter, and Klaus Müllen*

Max-Planck-Institut für Polymerforschung, Ackermannweg 10, D-55128 Mainz, Germany

Received September 22, 2000

Contents

I. Introduction

It sometimes remains unclear when looking at a discipline why a particular problem has in the past raised so much trouble and concern. Recalling the fierce debates on the usefulness of the aromaticity concept may suggest a somewhat frustrating conclusion: what remains is not so much the direct answer to the question but the chemical creativity which it has produced.[1] Whether or not we look at aromaticity as a structure or a property concept, a key question has always been whether it applies to any other molecule except benzene (**1**). Therefore, as one part of an aromaticity discussion, one can try to evaluate the wonderful manifold of conjugated and nonconjugated molecules originating from benzene as a unique building block. The coupling of benzene rings to biphenyl **(2)** or the fusion to naphthalene **(3)** are fundamental examples of this construction. When looking at **2** and **3** we are by no means confined to “nonnatural” chemistry since compound **4**[2] is a biaryl occurring in lignans and rifamycin **5**[3] is an ansa-type naphthalene. A further key question, when talking about the structure and properties of benzene, biphenyl, and naphthalene compounds, concerns the π-bonding situation, and this can be profoundly changed in a controlled way by electron transfer, i.e., by adding or removing electrons, or by complexation with metals.

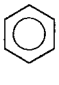

1

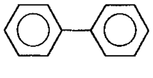

2

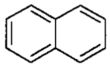

3

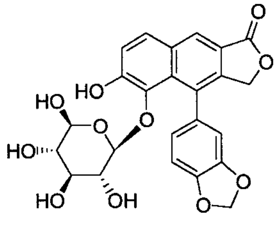

4

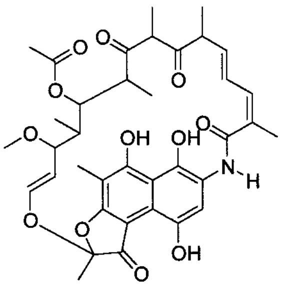

5

A crucial step of such a modular benzene chemistry is the stepwise buildup of higher homologues, i.e., biphenyl is the parent compound of a homologous series of oligophenyls **6**[4] while naphthalene gives rise to [*n*]acenes **7**.[5,6] Closely related to this design principle is the question of size dependence of properties. The electronic part of this question, which we will come back to later, is how electronic properties such as absorption wavelengths or redox potentials approach characteristic borderline values. The concept of homologous series has not only proven its value for chain-type conjugated oligomers, but also in classical aromaticity discussions; thus, the diatropism of [4*n* + 2]annulenes **8**,[7] higher homologues of benzene, has been followed as a function of ring size and the onset of olefinic behavior determined.

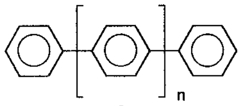

6

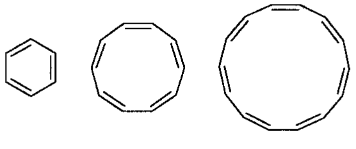

8

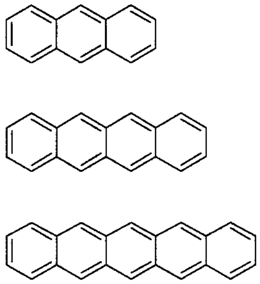

7

Many researchers in the organic chemistry of aromatic compounds tend to restrict their attention to “small” molecules typically containing the equivalent of a few benzene rings. Such structures are monodisperse, i.e., they possess a defined molecular

10.1021/cr990322p CCC: $36.00

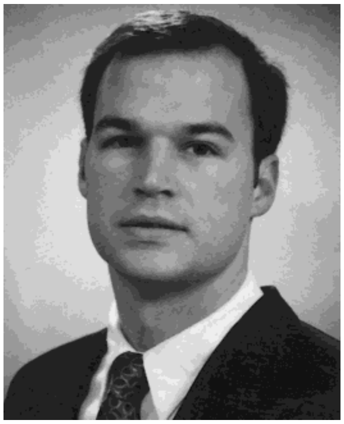

Dr. Mark D. Watson was born in Pascagoula, MS, in 1969. He obtained his B.S. degree in Polymer Science from the University of Southern Mississippi in 1992. He was awarded his Ph.D. degree in Organic Chemistry from the University of Florida, Gainesville, FL, in 1999. His research there in the group of Professor K. B. Wagener focused on utilization of olefin metathesis chemistry for the depolymerization of unsaturated elastomers and the synthesis of model polyolefin copolymers. In the same year, he joined the group of Professor K. Müllen to pursue postdoctoral research concerning the synthesis and phase behavior of discotic liquid-crystalline materials based on large polycyclic aromatic hydrocarbons.

Andreas Fechtenkötter was born in Georgsmarienhütte, Germany, in 1971. He received his B.S. degree from the University of Marburg in 1994 and his M.S. degree from the Technical University of Braunschweig in 1998. During this time, he spent two years doing research at the University of Utah, particularly in Professor P. J. Stang's group, for which he was awarded a DAAD scholarship. Since 1998, he has been working toward earning his Ph.D. degree at the Max Planck Institute for Polymer Research, Mainz, Germany, in Professor K. Müllen's group in the field of discotic liquid crystals.

Prof. Dr. rer. Nat. Klaus Müllen was born in Cologne, Germany, in 1947. He obtained a Diplom-Chemiker degree at the University of Cologne in 1979 after work with Professor E. Vogel. His Ph.D. degree was granted by the University of Basel, Switzerland, in 1972, where he undertook research with Professor F. Gerson on twisted π-systems and EPR spectroscopic properties of the corresponding radical anions. In 1972 he joined the group of Professor J. F. M. Oth at the Swiss Federal Institute of Technology in Zürich, where he worked in the field of dynamic NMR spectroscopy and electrochemistry. He received his Habilitation from the ETH Zürich in 1977 and was appointed Provatdozent. In 1979 he became Professor in the Department of Organic Chemistry, University of Cologne, and accepted an offer of as Chair in Organic Chemistry at the University of Mainz in 1983. He joined the Max-Planck-Society in 1989 as one of the directors of the Max-Planck-Institute for Polymer Research. In 1993 he was awarded the "Max-Planck-Forschungspreis" and in 1997 the "Philip-Morris-Preis". He has been a visiting scientist at the University of Osaka (JSPS), the University of Shanghai, the University of Leuven, and the University of Jerusalem. His current research interests focus on synthetic macromolecular chemistry, synthetic organic chemistry, physical organic chemistry, and material sciences. A crucial goal is the correlation of molecular structures and suprastructures with physical properties.

weight. This community has a natural reservation against polymers since in most cases—dendrimers[8] are a noteworthy exception—they represent a polydisperse mixture of different molecular weights and inevitably contain structural defects. It has been discussed at length that the view of polymer chemistry as being somewhat unreliable is, at best, historical.[9] Any aromaticity discussion will soon raise the awareness that benzene chemistry is a starting point for polymer chemistry and, in turn, that π-conjugated polymers contribute tremendously to theories of π-bonding structures.[10]

Comparison of cyclic π-systems with their isoelectronic linear analogues has always played an important role in π-bond theory. Interestingly, this concept has been extended to the description of conjugated polymers as well. Therefore, the repeat unit of the latter, e.g., a phenylene **6** or phenylenevinylene **9** group, is fused to a ring under formation of either a Hückel or Möbius topology (Figure 1), respectively, thus providing a surprisingly simple description of the band structure of the corresponding linear polymer. It should be noted at this point that elementary MO models are relevant for aromaticity discussions at different levels of sophistication. Typical cases are Hückel's rule or the theory of first- and second-order π-bond fixation. The description of conjugated polymers rests upon the linear combination of *molecular* orbitals of multiple repeat units, thus affording band structures. Therefore, the band gap between the valence and conduction band corresponds to the energy difference between the HOMO and LUMO and is relevant for optical absorption and photoluminescence behavior.

A prototype benzene-derived conjugated polymer is poly-*p*-phenylene (PPP) (**6**, *n* "large"), which for a long time has constituted a tremendous synthetic challenge due largely to limited solubility.[11] Synthesis and processing, i.e., creation of a defined macroscopic

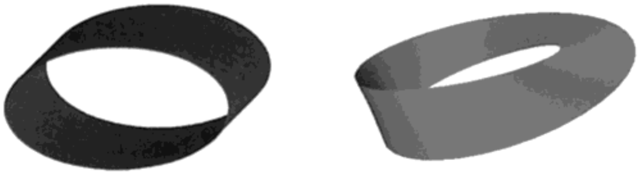

Figure 1. Hückel- and Möbius-type topology.

state of matter, must be tackled in a parallel approach; therefore, the solubility of PPP and its alkyl-substituted derivatives is not only relevant for structural elucidation, but also for device fabrication involving film formation by spin coating. In an analogous fashion, fused benzene derivatives such as oligoacenes lead to the corresponding polyacenes **7**[5,6] or, with a different topology, to polyrylenes **10**,[12,13] which have had an enormous impact on the chemistry of conjugated polymers with a low band gap.[14–16]

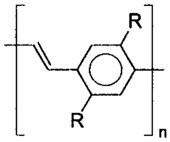

9

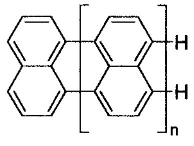

10

While the electronic design of conjugated polymers will appear to be an important concern below, it should be mentioned that benzene-derived polymers should be looked at not only from the point of view of extended π-conjugation. Other important aspects of introducing benzene units into polymers are the high chemical and thermal stability of the building block and its easy chemical functionalization. Thus, styrene synthesis by dehydrogenation of ethylbenzene is the starting point of polystyrene **11** synthesis, while polycondensation of terephthalic acid with glycol yields poly(ethylene terephthalate) (PET, **12**). The realization of the improved properties of poly(ethylene naphthalate) (PEN) has sparked R&D efforts devoted to practical synthesis of the requisite monomer(s) **13**.[17] Nucleophilic aromatic substitution reactions are involved in the formation of more rigid chain structures such as polyphenylenesulfide **14**,[18,19] while polyetherketones such as **15**[20,21] can be synthesized by both electrophilic and nucleophilic aromatic substitution reactions. Further, polycondensation of multifunctionalized benzene compounds such as tetraaminobiphenyl **16** affords heterocyclic polymers such as polybenzimidazoles **17**.[22,23] Structures such as **15** and **17** are termed high-performance polymers, for which chemical and thermal stability are key properties. Polymer **17** has recently been used as membrane material for fuel cells.[24,25]

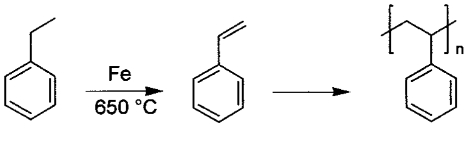

11

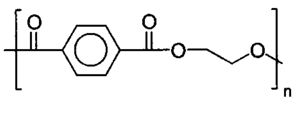

12

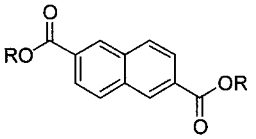

13

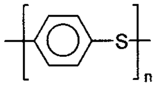

14

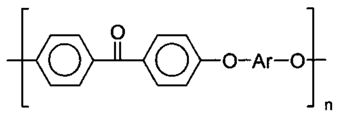

15

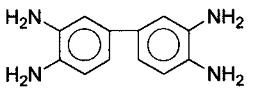

16

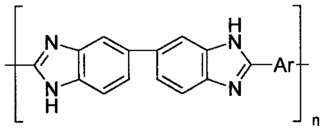

17

The past decade has led to the detection of new carbon allotropes such as fullerenes[26] and carbon nanotubes,[27,28] in which the presence of five-membered rings allows planar polycyclic aromatic hydrocarbons to fold into bent structures. One notes at the same time that these structures are not objects of controlled chemical synthesis but result from unselective physical processes such as laser ablation or discharge in a light arc.[29] It should be noted, on the other hand, that, e.g., pyrolytic graphitization processes, incomplete combustion of hydrocarbon precursors yielding carbon black, and carbon fibers[30] are all related to mechanisms of benzene formation and fusion to polycyclic aromatic hydrocarbons.

The above materials are useful in highlighting two further aspects of benzene-based chemistry, i.e., (i) transition from 2D to 3D structures and (ii) transition from macromolecular to supramolecular architectures. While already traditional benzene chemistry has proceeded from flat disc-type structures to double and multilayered cyclophanes such as **18**[31] and **19**,[32] graphite and its intercalation cannot be understood without considering layer formation. A closely related *supramolecular* case is the formation of discotic mesophases in which polycyclic aromatic hydrocarbons such as **20**−**22**, when decorated with flexible alkyl substituents, form anisotropic melts with stack-type arrangements of the disks (see Figure 2).[33] Also, the formation of carbomesophases in graphitization processes from pitch and thus the structural anisotropy of the final material rests upon the initial supramolecular ordering and subsequent cross-linking of disc-type polycyclic aromatic hydrocarbons.[34]

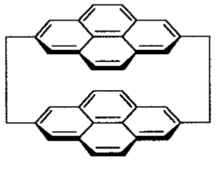

18

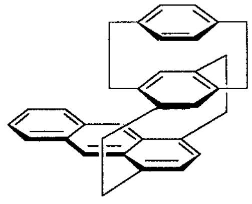

19

The present article is centered around macromolecular and supramolecular structures obtained upon use of benzene as a regular building block. While, e.g., the gas permeability of poly(ethylene terephthalate)s,[35] the mechanical strength of carbon fibers,[36] and the ion conductivity of polybenzimidazoles[24] are important features from a practical viewpoint, the focus here is on the occurrence of π-conjugation, or lack thereof, originating from the repetition of the aromatic benzene units in various structural motifs. If the reader regards materials

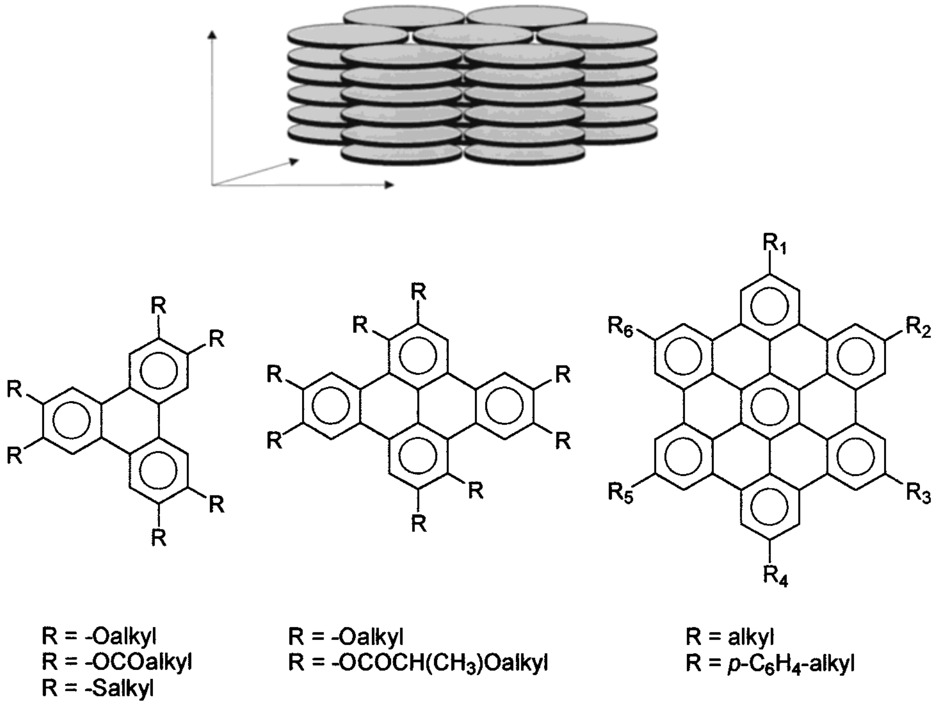

20 **21** **22**

Figure 2. Stack-type arrangement of a variety of discotic liquid crystals.

science as a sin against honest fundamental research, the authors ask for his/her forgiveness. It is true, however, that oligomers and polymers with extended π-conjugation serve as important active components of electronic and optoelectronic devices.[37] Therefore, charge-carrier processes often play a crucial role. Important ingredients of materials approaches are (i) the active physical function of a compound as part of a complex system, which is not revealed by just recording spectra, and (ii) the considerations of solid-state structures. While materials aspects are not within the attention of this text, there is no doubt that the bonding of extended oligomeric or polymeric π-systems, e.g., the transition from benzenoid **23** to quinoid borderline structures **24**, is an essential part of any aromaticity discussion.

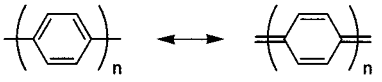

23 **24**

The controlled repetition of benzene rings by covalent and noncovalent bonding is also a means of producing nanosized structures in a systematic fashion. This is exciting because physics has more recently provided methods for the detection[38,39] (in real space) and direct manipulation of nanosized objects.[40-42] These could be particles such as, e.g., pigments or lattices, but also single molecular and macromolecular structures. It is quite remarkable, although not anticipated in the earlier benzene chemistry, that benzene-based macromolecular and supramolecular structures are particularly useful objects for nanoscience and even nanotechnology since they allow a straightforward transition between different length scales.

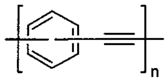

25

The following aspects will be addressed. (1) Conjugated polymers with benzene-derived repeat units (section II): typical examples are the already mentioned poly-*p*-phenylene (PPP) **6**,[43] polyphenylenevinylenes (PPV) **9**,[43] and polyphenyleneethinylenes (PPE) **25**.[44] Some typical questions are obvious: how do the aromatic or olefinic units interact via the formal single bonds and how far does an extra charge or an excitation delocalize over the chain. (2) Large polycyclic aromatic hydrocarbons (PAHs) as molecularly defined graphite subunits (section III): PAHs have long been recognized as ideal model compounds for π-bond theory. Therefore, the size, the topology of the ring fusion, and the periphery are crucial not only for the electronic discussion at a molecular level, but also for the packing of PAHs in both two and three dimensions. (3) Dendrimers from benzene repeat units (section IV): many flexible polymer chains form random coils, while, e.g., PPP exists as a linear rigid-rod structure. Monodisperse 3D macromolecules such as **26** with well-defined size and shape can be constructed from hyperbranched polyphenylenes.[8,45-64] The strong twist between neighboring benzene rings excludes any extended π-conjugation. However, incorporation of, e.g., dyestuff molecules produces new nanochromophores. (4) Single-molecule visualization of nanosized polyphenylenes and PAHs (section V): When characterizing chromophoric or electrophoric π-systems in the bulk, this process is dealing with ensemble properties. Detect-

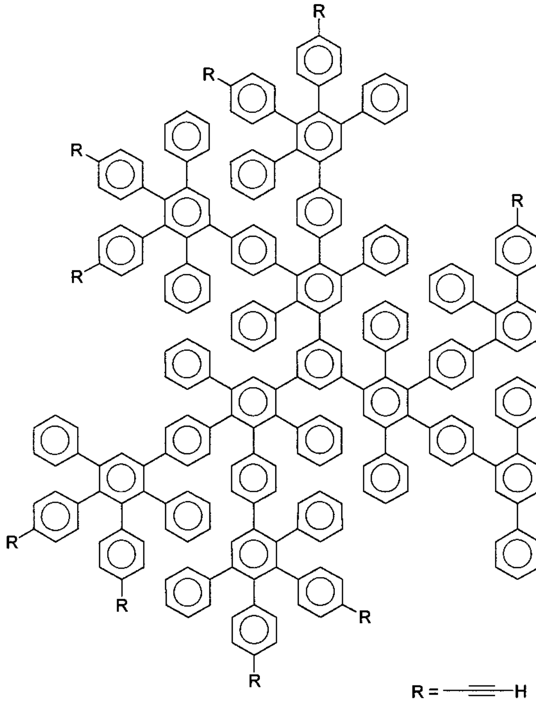

26

ing single-molecule properties,[38−40,42,47,65−67] however, leads to completely new functional concepts, and benzene-based compounds are particularly well-suited subjects for this developing technology. Here there is a synergism through which spectroscopic techniques are improved and in the course greater understanding of structure−property relationships is gained.

II. Conjugated Oligomers and Polymers

The subject contained herein has been recently reviewed,[4,37,43,44,68−71] and in particular, the subject of 'aromaticity' in polymers will be covered in another article within the current issue. Remaining within the theme of this article, we do not attempt by any means to comprehensively cover the subject but rather discuss some of the important consequences of incorporating benzene units into conjugated polymers.

PPP provides the simplest form of 1-dimensionally enchained benzene rings. The smallest oligomeric examples, biphenyl and terphenyl, achieve their lowest energy conformations calculated with torsion angles of 45° and 50°, respectively.[72,73] The molecular axis may be considered as a rigid rod bisecting the rings along the inter-ring σ bonds. The rigidity, planarity, and resulting properties of these and higher homologues, however, are a function of the state of matter in which they are observed as well as the molecular weight.[74] While intramolecular steric repulsion forces a torsion angle in isolated molecules, single crystals of oligophenylenes **6** yield structures in which this angle is at or near zero.[75] Intermolecular packing interactions overcome the intramolecular steric interaction forcing the rings into coplanarity, and this difference no doubt has drastic effects on the optical and electronic properties.

A naive consideration of the structures of high molecular weight conjugated polymers generally leads synthetic polymer chemists to describe these as "rigid" 1-dimensional objects. This continuously occurs even though we learn from the beginning that all molecules are subject to deformation. Simple IR characterization of aromatic compounds, for example, reveals out of plane bending modes. Long linear combinations of building units with such flexibility, though small on a local scale, should certainly lead to highly nonplanar structures on a larger scale. In particular, the effects of thermal motions in solution should produce increasingly more drastic manifestation with greater chain lengths. Therefore, high molecular weight, structurally well-defined linear polymers provide a good test case to evaluate the bonding situations.

Both empirical measurements[76−80] and theories applied in the polymer field have helped to confirm at least the physical manifestation of the flexibility of benzenoid and related conjugated structures. The challenge to understand the conformational properties of polymers has spurred a number of notable physical chemists to develop a field rich in theory.[81−83] One concept which has proven useful is a parameter, the persistence length (a), commonly used to describe the stiffness of polymer chains. In the case of a flexible species, the polymer chain may be described as a random coil with continuous curvature. If two tangents are drawn to the curve at a given distance, the angle between these two tangents describes the curvature. More specifically, the persistence length is the distance between two tangents whose directional correlation is reduced by a factor of 1/e. The shorter the distance at which this occurs, the more flexible is the polymer chain. For a true rigid-rod polymer, it goes without saying that this large degree of curvature would never be reached regardless of the chain length.

MD simulations of PPP **6** indicate that there is a large degree of flexibility attributed primarily to out of plane bending.[84] If the torsion angles between individual benzene rings were all held at zero, this would lead to a ribbon with curvature confined to two dimensions. However, it can easily be perceived that contributions from nonzero torsion angles in combination with the bending results in a 3-dimensional coil. From the simulated structures, the persistence length a was calculated to be 220 Å or 51 benzene rings, suggesting remarkable flexibility for this "rigid" polymer.[85]

Empirical studies[76−80] have born out this observation for conducting polymers utilizing typical polymer analytical tools including gel permeation chromatography, light scattering measurements, osmometry, viscometry, and small-angle X-ray and neutron scattering. Again, the need for well-defined and highly soluble polymers is emphasized, and this has been achieved in a number of cases through advances in synthetic polymer chemistry. In the case of a substituted PPP **27**[76] derivative, a persistence length of 126 Å (30 benzene rings) was determined. It was suggested that the persistence length might be decreased by steric repulsion of substituents in the "bay" positions of the polymer. Measurements on a polyphenylene ethynylene **28** revealed a persistence length of 300 Å or 20 repeat units (20 alternating benzene rings and triple bonds).[79] Calculations suggest that even 2-dimensional structures such as acenes and graphite-like sheets have this intrinsic flexibility and that truly rigid structures might only be obtained through bonding in 3-dimensions.[84] Experimental measurements on the ladder polymer **32** (to be discussed later), provide support for this prediction.[78] Remarkably, a persistence length of only 65 Å (~15 benzene rings) was determined for this ribbon structure.

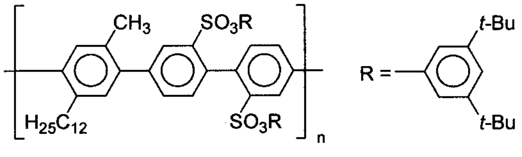

27

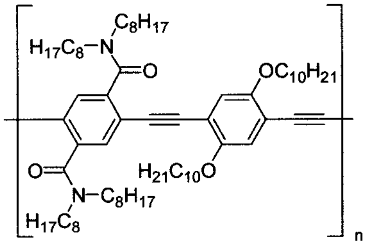

28

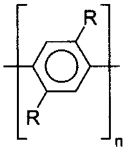

R = alkyl

29

Alkyl substitution as in **29** is of key importance for rendering oligo- and polyphenylenes soluble but causes significant torsion about the inter-ring bond (dihedral angles: PPP = 23°, 2,5-dialkylated PPP > 45°).[86] This will, of course, affect the conjugative interaction via these bonds and the size dependence of the electronic properties.[87−90] Cyclic voltammetry reveals that methyl-substituted oligophenylenes **30** and **31** behave as separate electrophores with about one-half the chain length.[91] An important concept here is the introduction of saturated bridges between the two ortho-positions. Particularly remarkable are the so-called ladder polyphenylenes[92] **32**[93,94] and their related oligomers in which neighboring benzene rings are linked by one methylene bridge (fluorene subunit), providing a more planar extended π-system. The additional advantage of such structures is that solubilizing alkyl chains can be attached to the sp^3-carbon bridges without causing an inter-ring torsion, giving rise to soluble and thus solution processable polyphenylene analogues.

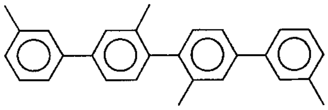

30

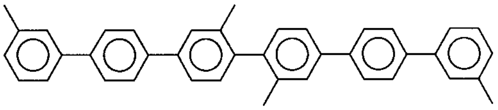

31

A structural compromise between the fully bridged ladder system and the parent polyphenylene are stepladder polyphenylenes in which repeat units, such as fluorene, indenofluorene, or tetrahydropyrene, are linked by single bonds giving rise to polymers **33**,[95−100] **34**,[101−103] and **35**,[104] respectively. The resulting π-chains, of course, possess a typical biphenyl torsion angle between the repeat units. Polyphenylenes have a relatively large energy gap, which explains their behavior in photoluminescence and electroluminescence as blue emitters.[105]

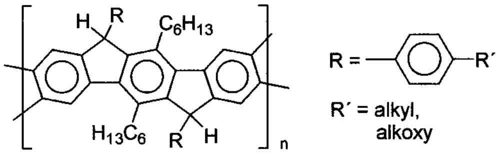

R′ = alkyl, alkoxy

32

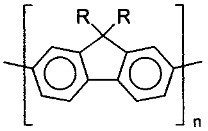

R = alkyl

33

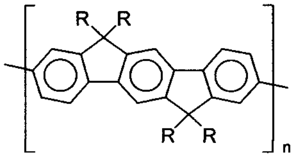

R = alkyl

34

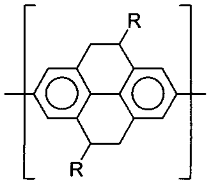

R = alkyl

35

When talking about optical, electronic, or optoelectronic properties, a good case can be made by plotting a measured property of monodisperse oligomers versus the reciprocal number of repeat units and thus monitor how oligomers approach the behavior of the corresponding polymer. This concept has led to the definition of an "effective conjugation length",[4,106−111] a reality which falls short of the idealized "fully conjugated" high molecular weight polymer. This can be defined, for example, as the oligomer chain length at which the λ_{max} value no longer changes with added repeat units and approximates that of the corresponding polymer. Other properties, such as redox potentials, can be used as well. A polymer analogue of aromaticity, the concept is a bit ethereal and elusive, where drastically different values may be obtained depending on the method of assessment.[4] Although lacking a firm theoretical foundation, the concept of effective conjugation length has proven extremely useful in analyzing conjugational effects between benzene repeat units in chain-type structures. Possible explanations for the convergence of optical properties are torsional effects and high degrees of bond alternation along the chain. The prerequisite for this type of treatment is, of course, the availability of pure, defect-free series of oligomers.

For example, the optical absorption energies obtained from the longest wavelength absorption maxima were plotted versus the inverse chain length for the polyphenylene derivatives PPP **6**, PTHP **35**, and LPPP **32**, and a linear relation was seen in all cases.[112] Prediction of the effective conjugation length for PPP, however, remained elusive due to the absence of an exact experimental value for high molecular weight pristine PPP in solution. The most interesting outcome is that the effective conjugation length determined for the LPPP **32** was ~11−12 benzene rings compared to ~20 rings for the PTHP **35**; i.e., the optical properties converge much more rapidly to those of the respective polymer in the highly planarized system.

In a related study[106] concerning oligomeric PPV (**9**, R = alkoxy), a plot of absorption energy versus reciprocal chain length deviated from linearity at longer chain lengths and the extrapolated energy ($E_{1,\infty}$) was significantly different from the known value for high molecular weight polymer. After finding that exponential growth functions of absorption data versus the chain length provided a much better fit, these nonlinear relations were applied to a number of conjugated oligomers. Equally good fits were seen for other oligoarylenes, oligoarylene−vinylenes, and oligoarylene−ethynylenes including those containing analogous (het)arylene units. Evaluation of the data in this way allowed the comparison of a number of effects including heteroatoms, enchained double bonds versus triple bonds (greater bond alternation in the latter), and sterics. Further, the ECL for PPP **6** was determined by this method to be between 9 and 11 benzene rings.

Tuning the wavelength of emission in photoluminescent and electroluminescent polymers as active components of light-emitting diodes has been an important concern.[37,70,113−119] As anticipated from a simple molecular orbital model, the optical transition energy becomes smaller when proceeding from biphenyl **2** to stilbene **36**; homologous series of oligophenylenes **6**, oligophenylenevinylenes, and corresponding polyphenylenevinylenes **9** have, therefore, played an important role in LEDs. Not surprisingly then, arylenevinylene chain structures **37**,[120,121] in which the length of the oligophenylene moiety can be varied, bridge the gap between PPPs and PPVs.

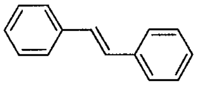

36

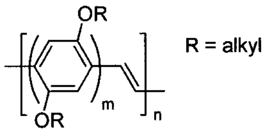

37

We have so far not specified whether photoluminescence data are measured for solutions or the solid films (these should be amorphous in order to avoid light scattering effects). Light emission in a device requires the presence of solid materials, a feature which has profound effects on the optical properties and highlights, again, that in dealing with materials properties one cannot restrict the attention to the behavior of separate molecules in isolated solution. Photoluminescence spectra measured for films often show additional bands having a bathochromic shift with respect to those of the solution. The question of whether this is the result of ground-state aggregation or excimer formation has long been debated in the literature.[122] The interaction between π-systems in the solid state can lower the relevant energy gap. Thus, even if aggregate formation only involves a minor part of all the molecules, energy transfer leads to a situation in which the emission characteristics are controlled by components with lower energy gaps.

The need for taking into account intermolecular conjugational effects is further highlighted by the fact that in an electroluminescent device holes and electrons which are injected at the electrodes have to migrate through the films, and this transport is, again, depending upon the packing and eventually the formation of ordered arrays of the conjugated chains.[123] Although this is beyond the purpose of this text, it should be mentioned that solid-state structures originating from side-by-side arrangements of linear polyphenylene chains, both in the bulk and on surfaces, have attracted great interest.[124−127] As part of this supramolecular organization of polyphenylenes, we have synthesized rod−coil block copolymers **38**, **39**, and **40** with conjugated polyphenylenes serving as the rigid-rod part.[128] Different polymers such as rigid rods and coils tend to undergo phase separation in the solid state and are driven into nanophase separation if the blocks are covalently linked. Accordingly, the presence of a flexible coil component can be relevant for achieving supramolecular organization and thus affecting intermolecular π−π-interaction between the rigid-rod portions of the polymers.

Conjugated oligomers and polymers with much lower energy gaps than, e.g., PPP **6** and PPV **9**, so-called low-band gap materials,[129] have attracted great attention because they are important not only for achieving absorption and emission bands with a strong bathochromic shift eventually in the NIR range, but also for influencing electrical conductivity and nonlinear optical properties. While the intact benzene ring is normally associated with a high energy gap, transition to a quinoid structure is supposed to lower the energy gap.[130] Thus, tetraphen-

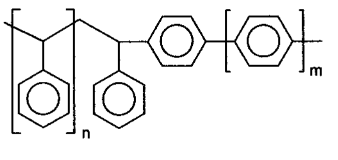

38

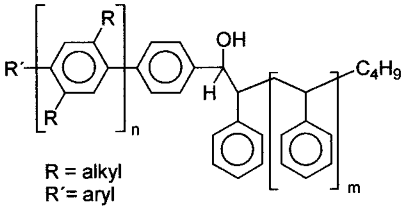

39

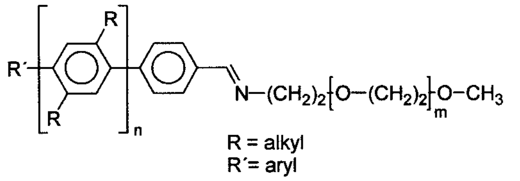

40

ylquinodimethane **41**[131] and its indenofluorene-derived analogue **42**[132] are violet compounds. The polymer chain in **43**[133] consists of an alternating array of benzenoid and quinoid subunits and, thus, possesses a degenerate ground state as is the case in polyacetylenes. UV–vis absorption spectra of this polymer indicate the presence of the desired quinoidal units. Unfortunately, the material contains structural defects (nonquinoid) and, not surprisingly, is chemically unstable. Alternately, an analogue containing alternating 1,4- and 1,3-phenylene units has been prepared **44**.[132,133] Due to the 1,3-linkages, localized phenylenemethide units are obtained with limited interaction along the chain. Another way of lowering the band gap is to induce significant torsion about exocyclic double bonds as nicely documented in the bisindenyl systems **45**[134] and applied to the polymer field in polymer structure **46**.[135] It is highly possible that quinoid states (right structure) contribute to the electronic ground state, reducing the band gap energy. In fact, this polymer displays the lowest energy gap ($E_g \approx 1.55$ eV) known for a well-defined neutral hydrocarbon polymer. The longest wavelength absorption is shifted into the NIR up to 799 nm. Surprisingly, high chemical stability is observed unlike that seen in other conjugated polymers with low band gap energies. In polycyclic π-systems made upon fusion of benzene rings, the particular topology is crucial for the energy gap. This will be considered in section III.

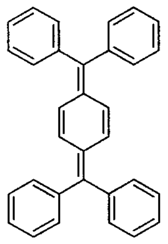

41

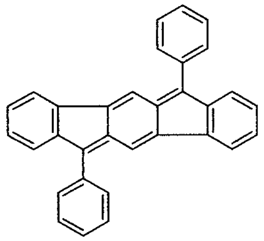

42

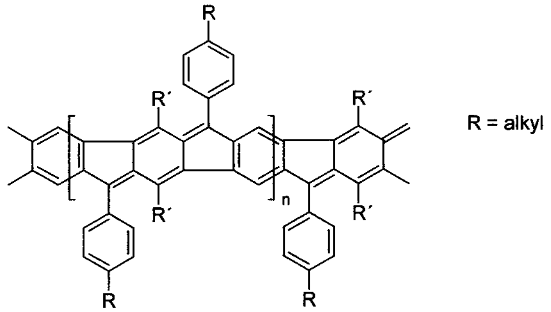

43

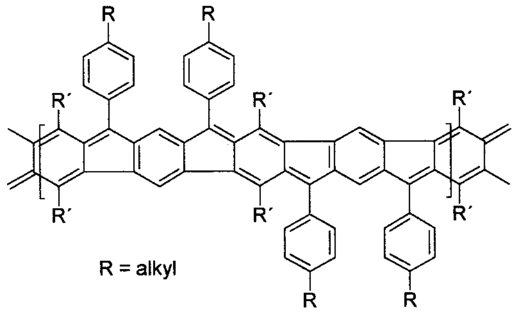

44

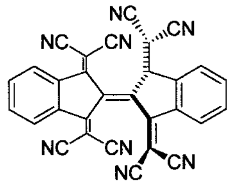

45

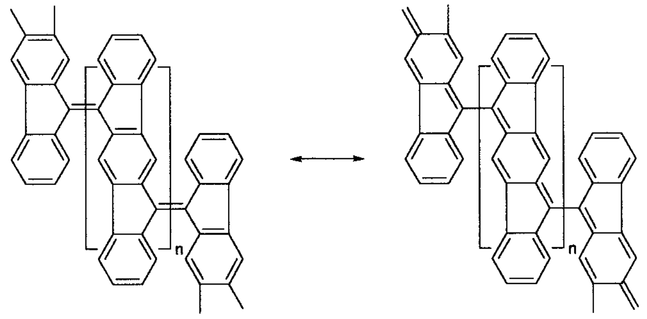

46

The major obstacle in the creation of low band gap oligomers and polymers is the increasing chemical reactivity, as observed in the attempted synthesis of **43**. Thus, increasing the size of oligo[*n*]acenes **7** causes tremendous stability problems.[136,137] A typical case is pentacene, which has served as an important semiconductor component in field-effect transistors (FETs), as FETs made with pentacene single crystals have shown a remarkably high charge-carrier mobility. One concern is to achieve a packing in the solid state suitable for charge-carrier transport. The other concern is to avoid oxygen during the processing since O_2 would immediately lead to destruction of the π-system. A precursor route has been worked out for the deposition of pentacene films in FETs, whereby the processing stage is achieved prior to formation of the unstable target.[138] This procedure involves spin coating of thin films of a precursor, from which retro-Diels−Alder reaction in the bulk state gives the desired pentacene films.

A large energy gap between the valence band and the conduction band in PPP **6** explains why the material is an electrical insulator, since there are no mobile charge carriers available. The formation of charge carriers is possible by partial oxidation or reduction. Such electron-transfer processes produce ionic species, which in the language of chemistry are described as radical anions or radical cations and as polarons in the language of condensed matter physics. The polaron is, in a sense, a radical anion plus the corresponding lattice distortion, and this is, indeed, very similar to what organic chemistry describes as electron-transfer-induced conformational changes. Transition from a radical anion to a dianion upon a second electron transfer is, of course, hampered by electrostatic repulsion, but the example of cyclooctatetraene shows[139] clearly that structural changes can, at least, partly overcompensate the electrostatic repulsion so that in an extreme case an electron transfer can even facilitate a second one. An important question in describing the successive electron transfers to or from an extended conjugated chain is the transformation of paramagnetic into diamagnetic molecules with antiparallel spins and, thus, singlet structures (note, again, that a bipolaron is a dianion plus the corresponding lattice distortion), and the transition between polarons and bipolarons would, indeed, influence the nature of the charge carriers in the conduction process. Here again, the problem of the extension of a polaron or dianion can be translated into the question how many repeat units of an oligophenylene or oligophenylenevinylene chain are involved in the delocalization of one or two extra electrons. In a similar fashion, an exciton can be described as being localized to only a part of a conjugated chain.[140]

In a band structure model, the partial oxidation or reduction of an extended π-system is described as creating new electronic states in the original band gap (mid-gap states), a process which is, of course, closely related to the creation of charge carriers.[140] The other reason this process is mentioned here can be seen from a simple description of, e.g., terphenyl, according to formula **47**. This description indicates an increasing contribution of quinoid structures with a formal double-bond character of the inter-ring bonds upon charge formation. It is the “defect” at the terminal *para*-position, which induces a “dearomatization“ process and increases the conjugative interaction across the inter-ring bonds together with the decrease of the energy gap. It should be noted that the alternative description of benzenoid **23** and quinoid **24** borderline structures of conjugated polyphenylenes is normally made for an infinite chain. In real molecules the nature of the end groups becomes important. Thus, a quinoid structure can be brought about not only by the charging process, see above, but also by the introduction of a sp^3-center according to formula **48**.[141]

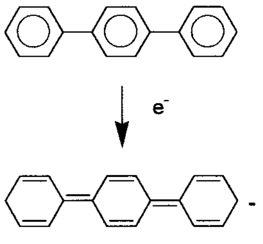

47

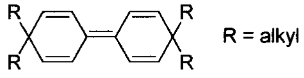

48

We have so far looked into the relative importance of benzenoid and quinoid structures in conjugated polymer chains as part of a more general discussion of aromatic versus nonaromatic structures. It is interesting, therefore, that structural concepts of organic chemistry parallel those of condensed matter physics. For a more detailed discussion, however, the reader is recommended to consult the specialized literature.

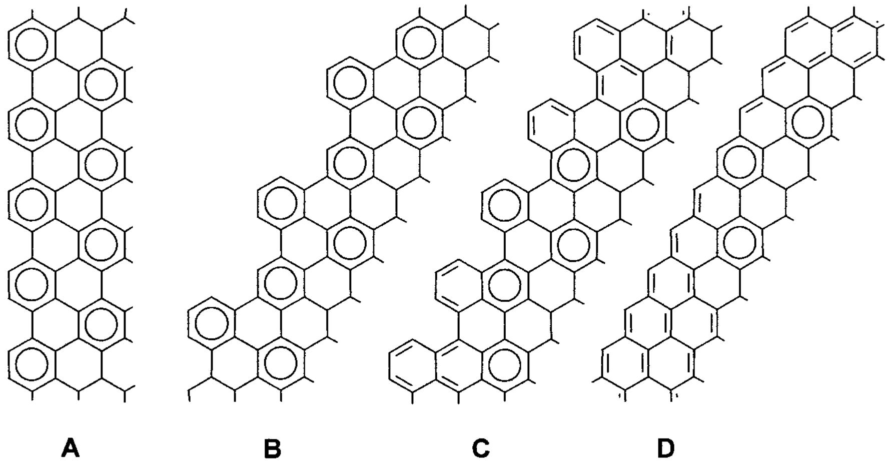

Figure 3. Peripheral topologies of large PAHs: (A and B) all-benzenoid, (C) acene-like, (D) quinoidal.[153,154]

III. Polycyclic Aromatic Hydrocarbons (PAHs)

A. Design and Synthesis of PAHs

There are two reasons to proceed from linear polymer structures such as **6** and **7** to polycyclic aromatic hydrocarbons (PAHs). Transition from systems with one translational period to systems with two translational periods is supposed to bring about a profound change of the electronic structure, and PAHs have, indeed, been among the oldest test cases of elementary π-bond theory.[142,143] Issues which have been addressed when evaluating the aromaticity of a given system have been *diamagnetic exhaltation, degree of alternation of bond lengths, planarity, chemical stability, and susceptibility to aromatic substitution*.[7]

One must be aware that among the polycyclic aromatic hydrocarbons, the all-benzenoid analogues constitute only a small subgroup. Thus, from the total of roughly 20 600 possible alternating hydrocarbons having between 4 and 10 fused benzene rings, only 17 are all-benzenoid.[142,144] If we restrict the attention to polycycles only made from six-membered carbon rings, the "benzene-like behavior" can adequately be described in terms of Clar's model of the aromatic sextet.[143] In this qualitative although highly successful concept the π-electrons are assigned to specific six-membered rings in such a way that the largest possible number of π-electron sextets is formed. If, according to the Clar formula, all π-electrons are distributible in closed sextets, the number of carbon atoms necessary is an integral multiple of six. *In the remainder of this text, the all-benzenoid PAHs will be distinguished as* PBAHs. The smallest example of a PBAH is the tetracyclic triphenylene **20** (R = H),[145,146] and a good case can be made when comparing triphenylene with its *cata*-condensed isomers [4]helicene **49**, chrysene **50**, benz[*a*]anthracene **51**, and naphthacene **52**.[142,147] Triphenylene possesses a lower chemical reactivity and a higher thermodynamic stability and within a molecular orbital description triphenylene is identified as having the largest resonance energy, the first ionization energy, and the largest HOMO−LUMO gap.[142] Therefore, while triphenylene is colorless, naphthacene is orange. Here again, the above concept of homologous series may be invoked since transition from naphthacene to pentacene causes a bathochromic shift of the long wavelength absorption maximum by 102 nm (in pyridine).[148−150] A related case is that of the oligorylenes **10**, where one proceeds from the yellow perylene to the red terrylene, the blue quaterrylene, and the green-black pentarylene.[151,152] The as yet

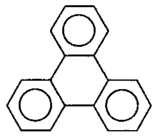

20

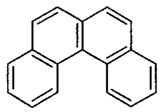

49

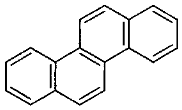

50

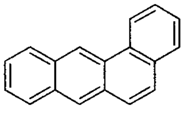

51

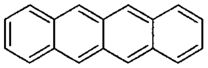

52

Scheme 1

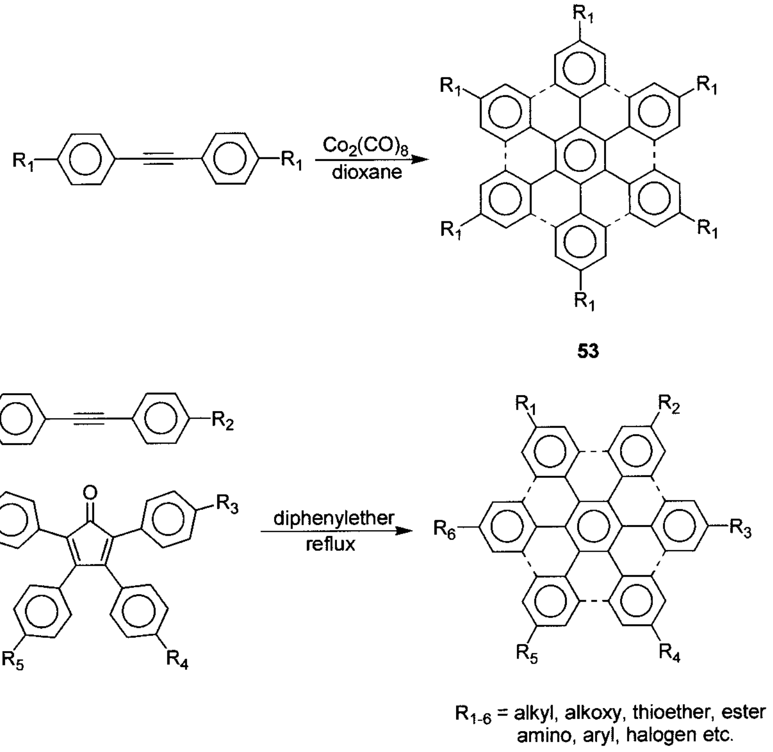

Scheme 2

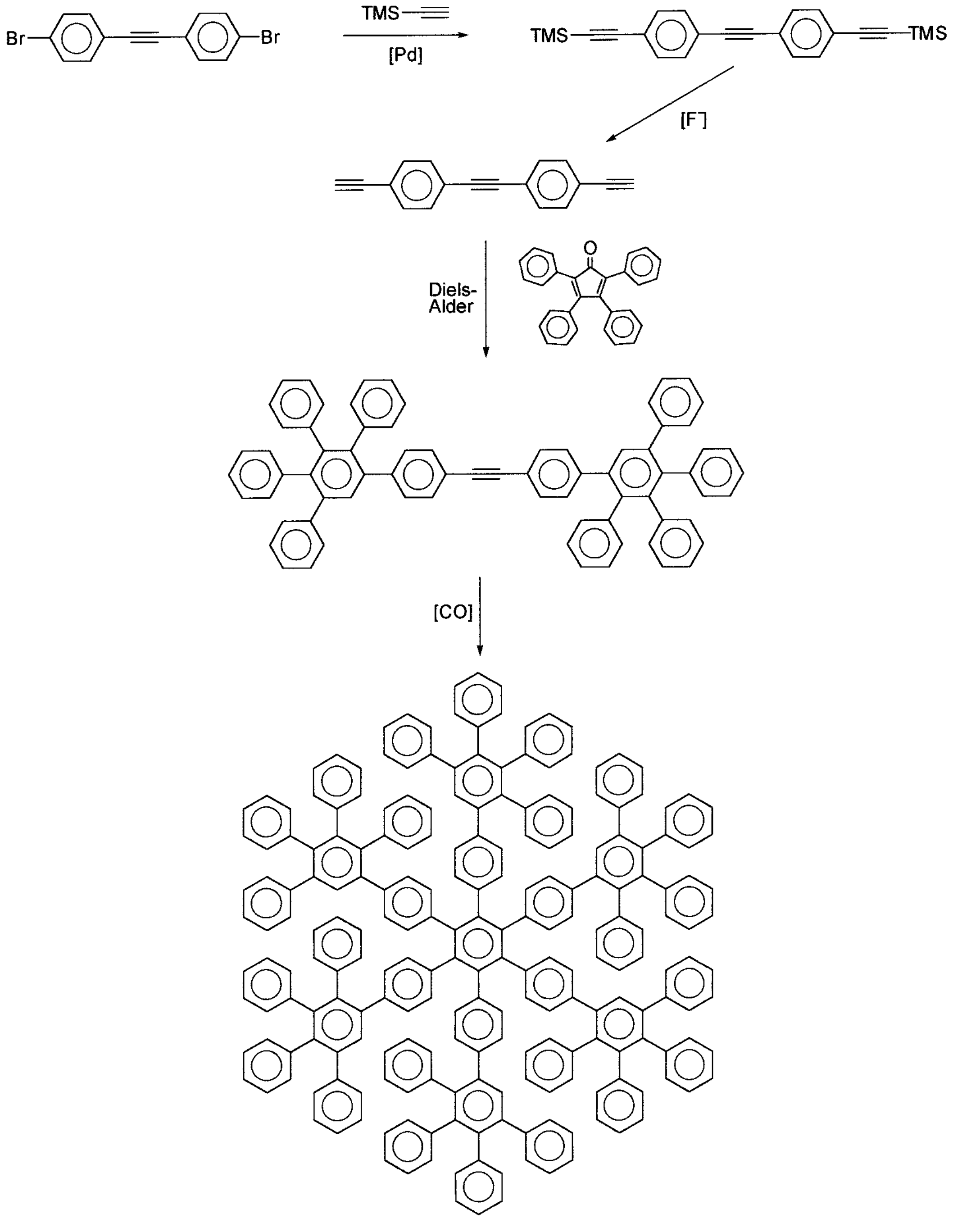

54

unknown high polymeric analogue of the rylenes is predicted to be a low band gap polymer.

Within the Clar-type topologies, one, of course, expects a lowering of the HOMO–LUMO gap upon increasing the size of the molecules. However, even if attention is restricted to benzene-related hexagonal structures, it must be pointed out that the π-bond structure and, in particular, the HOMO–LUMO energy gap of PAHs depend not only upon the size, but also upon the nature of the periphery (Figure 3, structures A–D).[153,154] In particular, a zigzag periphery is predicted to lead to a lower HOMO–LUMO gap than the armchair periphery.[153,154] It might be added that in nanotubes the occurrence of armchair configurations leads to metallic structures while zigzag structures give rise to semiconductors. Looking in somewhat greater detail at the linear peripheral topologies (see Figure 3), as occurring at the edge of a graphite layer, one clearly notices that A and B are all-benzenoid whereas C is acene-like and D possesses quinoid subunits. We are thus, again, confronted with the alternative of benzenoid versus quinoid structures, which has already occurred in describing linear polyphenylenes. This raises the question of the chemical reactivity of edge structures. Indeed, the formation of graphite-related structures at high temperatures is believed to form so-called “dangling hybrid orbitals” at the edges (possibly carbenes or radicals). These may be considered as half-occupied nonbonding molecular orbitals with

Scheme 3

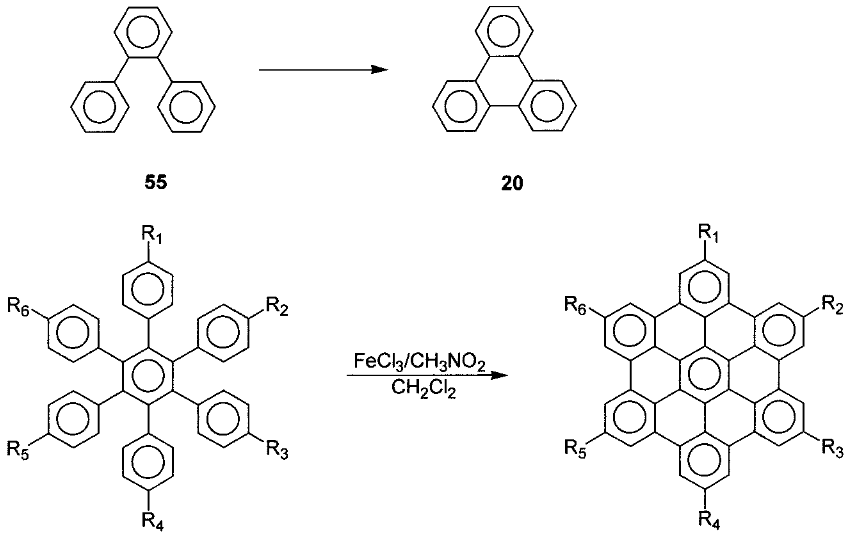

Scheme 4

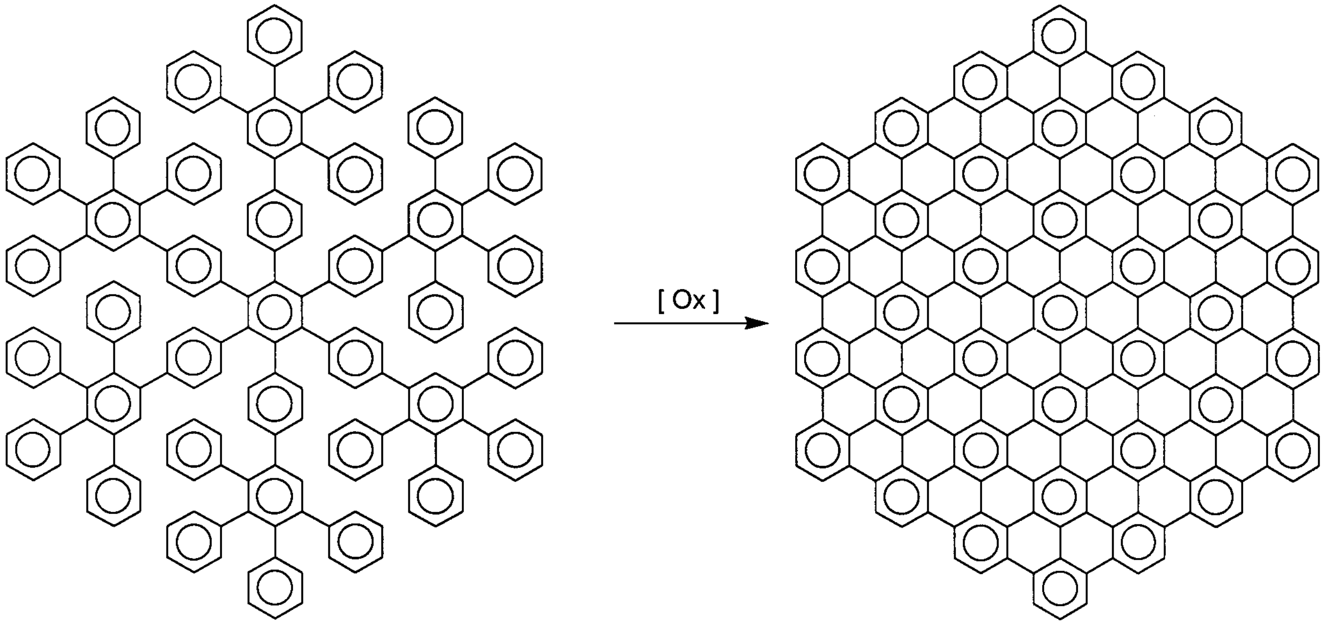

mid-gap energy levels. These can, of course, react with oxygen, producing various defect structures. These are typically ignored by solid-state physicists while dealing with the ideal, infinite sheets in graphite.

The number of possible PAHs which have been prepared, and/or strictly isolated, is relatively small compared to other classes of hydrocarbons.[142,147] One limiting factor is the harsh synthetic conditions which are often employed.[142,147] A particularly mild and reasonably well-defined synthetic method has been recently developed,[155−157] by which triphenylene-based, i.e., Clar-type PBAHs of unprecedented size become available.[46] The synthetic route taken is surprisingly simple and allows a systematic variation not only of the size, but also of the symmetry and the type of periphery.[158] The first phase of the sequence includes the synthesis of 3-dimensional oligophenylene precursors, which, due to the twisting among the benzene rings, are noncolored and nicely soluble (Scheme 1). It can easily be seen from the 2D representation that these structures are scaffolds that can meet the requirements for Clar PBAHs if all interior carbons are joined by single bonds (indicated by dashed lines in Scheme 1). This can be accomplished by mild oxidative cyclodehydrogenation at room temperature.[157] The requisite 3D oligophenylenes are available by transition-metal-catalyzed cyclotrimerization of suitable diarylacetylenes or by the Diels−Alder reaction of such diarylacetylenes with tetraarylcyclopentadienones with in situ decarbonylation.[158] The repetition of these reactions and the use of oligomeric starting compounds with multiple acetylene (dienophile) and cyclopentadienone

Scheme 5

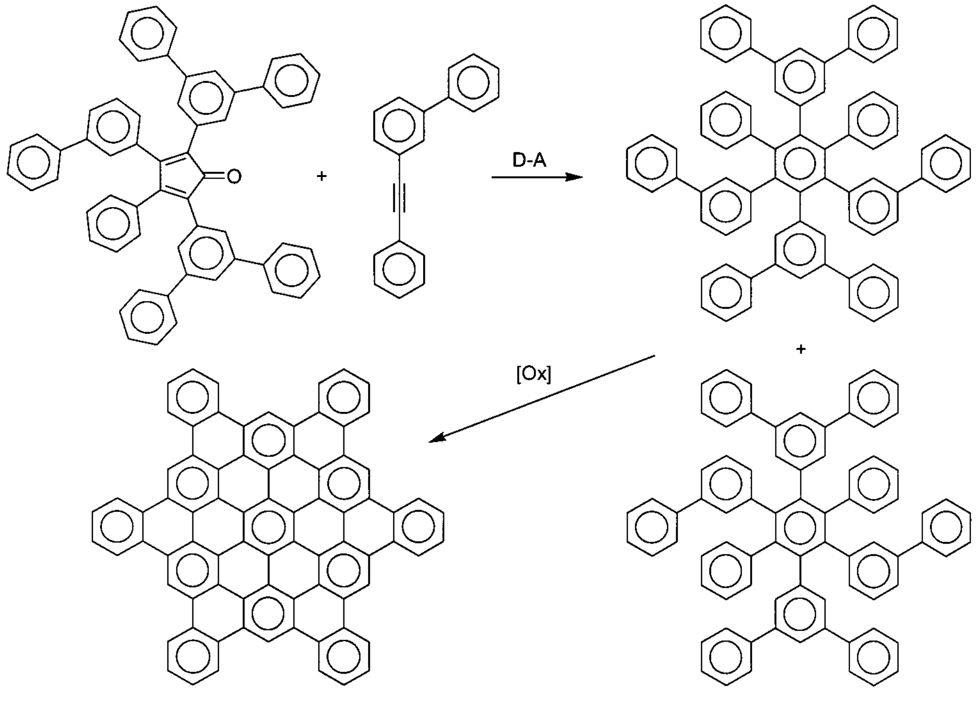

61

(diene) functions leads to a remarkable structural manifold (Scheme 2).[45] The topology of the oligophenylenes is designed such that the previously mentioned intramolecular dehydrogenation leads to a flattening of the molecule and the transition from an oligophenylene to a Clar-type PBAH. The prototype reaction is transformation of *o*-terphenyl **55** into triphenylene **20**, [145,146] and a particularly convincing case is the cyclodehydrogenation of hexaphenylbenzene **53** (R = H), readily available from diphenylacetylene, into hexa-*peri*-hexabenzocoronene **22** (**HBC**, R = H),[159] which proceeds in nearly quantitative yield (Scheme 3). Scheme 4 convincingly reveals the power of the above cyclodehydrogenation route.[160] The number of PBAHs which may be prepared this way is virtually unlimited by typical synthetic constraints, and significant strides toward the preparation of a library of such species have already been made. The value of such a library of structurally pure compounds in the study of the effect of geometry, size, periphery, etc., is self-evident.

The resulting PBAHs are more or less insoluble in organic solvents, which limits purification and renders spectroscopic characterization difficult. The same approaches to solubilization of rigid 1D polymers have been applied here, i.e., the attachment of flexible side chains, allowing full spectral characterization in solution in many cases.[155,161] Further, inclusion of these substituents modifies the materials properties in a dramatic fashion, yielding a novel class of liquid crystalline compounds[157,158,161] where the PBAH cores serve as the rigid element.

Some synthetic aspects of the above cyclodehydrogenation reaction are truly remarkable: (1) MALDI-TOF spectrometry proves that, indeed, 108 hydrogens are removed upon transition from **54** to **56** and that the resulting organic material is 99% pure;[160] (2) even strong steric hindrance of substituents can be overcome with the formation of nonplanar PAHs, which can be seen from the formation of dodecamethyl and the octadecamethoxy derivatives of HBC **57**[162] and **58**;[163] (3) solubility can be further improved by proceeding from [*n*]alkyl to branched alkyl substituents (compare **22** (R = *n*-$C_{12}H_{25}$)[155] and **59**)[164] or by introducing additional phenyl substituents as in

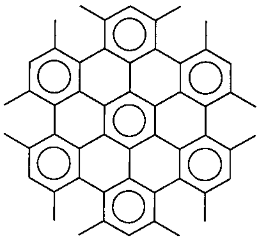

57

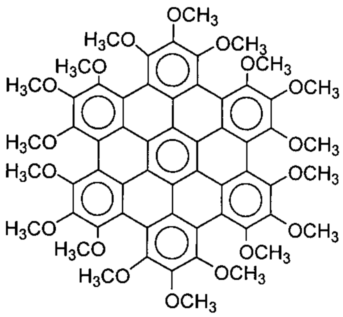

58

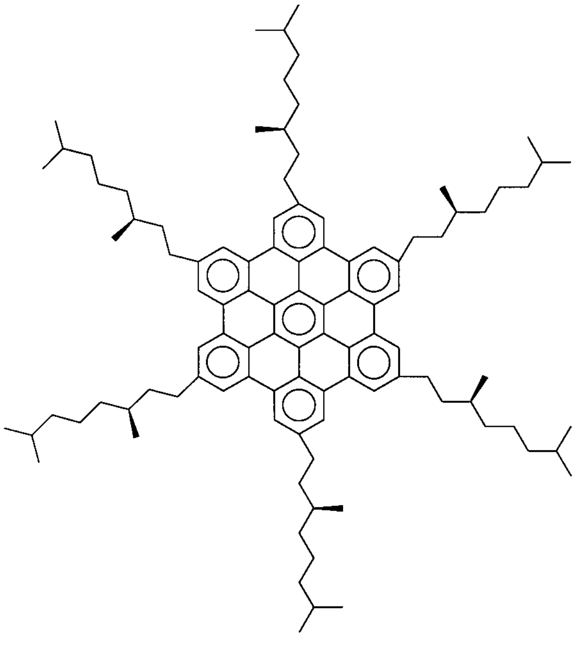

59

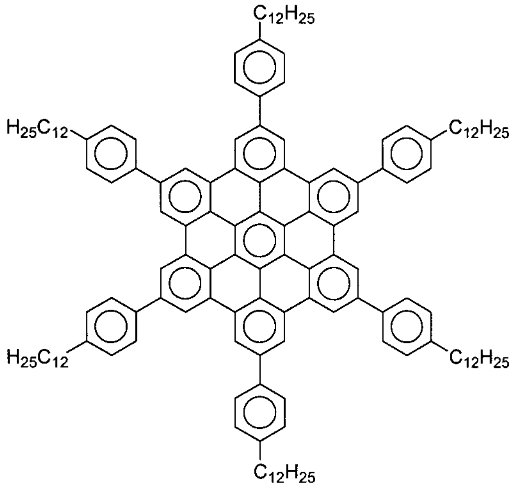

60

60.[157] This increase in solubility allows the study of solvatochromic effects in a broader range of solvents. Further, the phase width for LC behavior is widened to include lower temperatures, and these materials are pliable at room temperature, features which are important for device applications. (4) A systematic variation of the symmetry becomes possible by a design process, which, in a formal sense includes the fusion of further six-membered rings. Thus, hexabenzocoronene with a complete armchair periphery can be compared with its higher homologues **61** and **62** containing cove-type areas.[153,154] A homologue of HBC, which only contains a cove-type periphery and in which the hexagonal symmetry is maintained, is structure **61**, whose synthesis via combination of specifically substituted tetraarylcyclopentadienones and arylacetylenes is shown in Scheme 5. (5) Regarding the hexabenzocoronene as a large hexagon, a

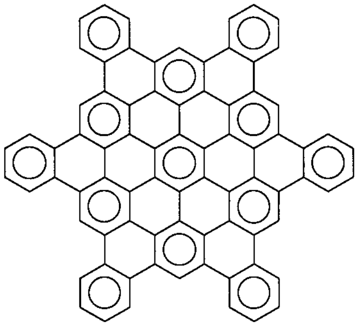

61

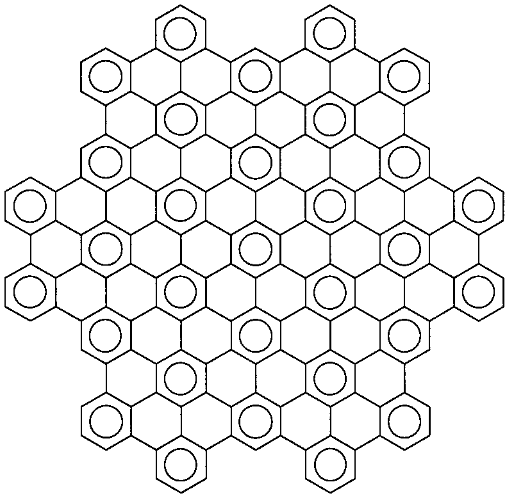

62

"superbenzene", one can readily synthesize polycycles which can be regarded as, e.g., supernaphthalene **63**[160] or supertriphenylene **64**[160] (see also section III.4).

B. Spectroscopic Characterization of Large PAHs

The structural identity of the giant PAHs, which has been mentioned already, can be deduced from MALDI-TOF MS, which even allows one to determine the exact masses. Further, spectroscopic characterizations, such as by Raman spectroscopy, have been performed[165] but are beyond the scope of this text. ^{1}H NMR spectroscopy and, in particular, the detection of ring-current effects has emerged as one of the most important methods for characterizing aromatic compounds and providing criteria of aromaticity.[166−168] We leave it to other articles in the current issue to review assessment of 'aromaticity' by NMR techniques, while we focus on some special circumstances which arise when characterizing large PBAHs by NMR.

A major obstacle in the NMR-spectroscopic description of PBAHs, related to the limited solubility, is the strong tendency of the disc-type structures to form aggregates in solution,[169,170] which causes significant line broadening and shielding. The shielding in this case is of course intermolecular, versus the diatropic effects[171] which are normally considered when looking

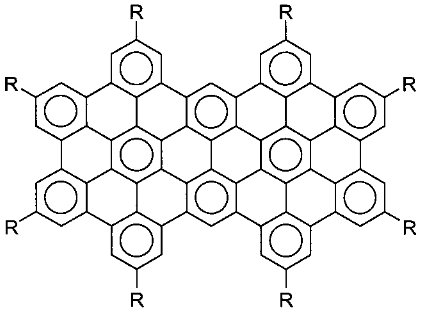

63 R = H, R = *t*-Bu

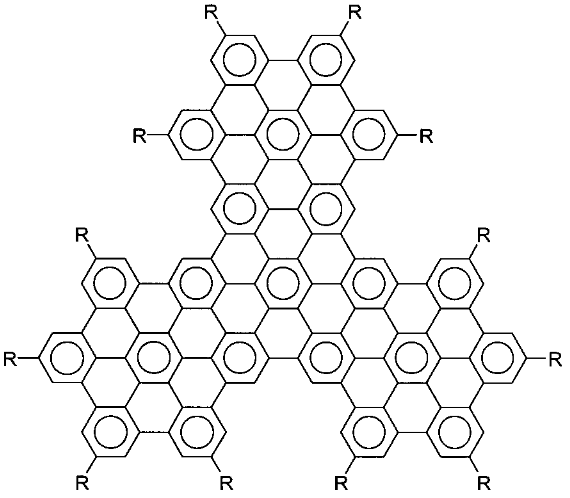

64 R = H, R = *t*-Bu

at single aromatic molecules. Figure 4 shows, however, that by increasing the temperature from 298 to 450 K, one can obtain ^{1}H NMR signals with sufficiently narrow line widths.[157] In a more detailed study one can observe the strong influence that changes of temperature and concentration have on the $\pi-\pi$-interaction of these aromatic compounds. The shifts of the aromatic ^{1}H resonance frequencies dependent on changes in temperature are depicted in Figure 5 and on concentration in Figure 6.[172] As can be seen in Figure 5, upon heating, the relevant aromatic signals experience a downfield shift of $\Delta\delta = 0.26$ from $\delta = 8.11$ ppm to $\delta = 8.37$ ppm. A somewhat less pronounced shift to low fields can be observed for the α-CH_2 protons of the alkyl side chains. Likewise, decreasing the concentration from 51.2×10^{-3} to 1.4×10^{-3} mol/L results in a shift to low fields by almost 0.5 ppm. Again, a less pronounced shift to low fields can be observed for the α-CH_2 protons of the alkyl side chains. It can be summarized that increasing temperature and decreasing concentration are affecting the solution behavior in a way that smaller aggregates are formed. This results in a shift of the aromatic proton signal toward lower fields, which is totally in line with the theoretical value calculated for an isolated molecule (see below).[173,174] On the other hand, at this point it cannot experimentally be accomplished to reach concentrations low enough to measure isolated HBC molecules in solution, which would give the possibility of determining association constants and ring-current parameters.

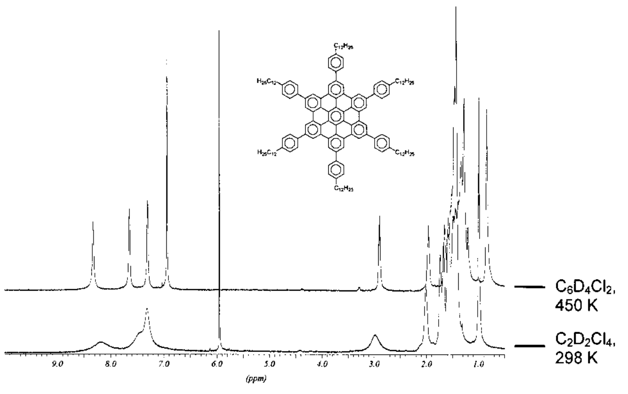

Figure 4. Temperature dependence of the line widths of HBC-PhC_{12} **60**.

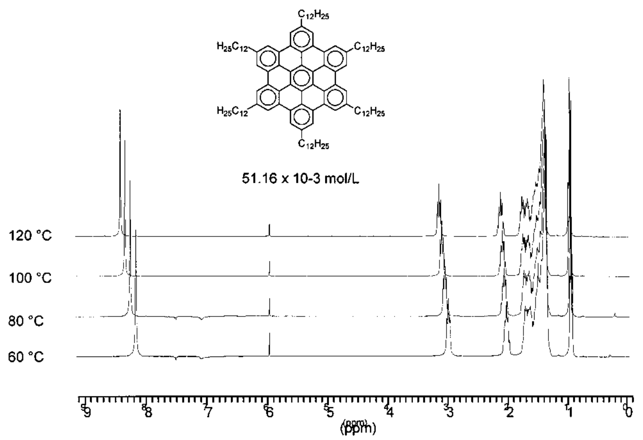

Figure 5. Temperature-dependent ^{1}H NMR spectra of **22** ($R_{1-6} = C_{12}H_{25}$).

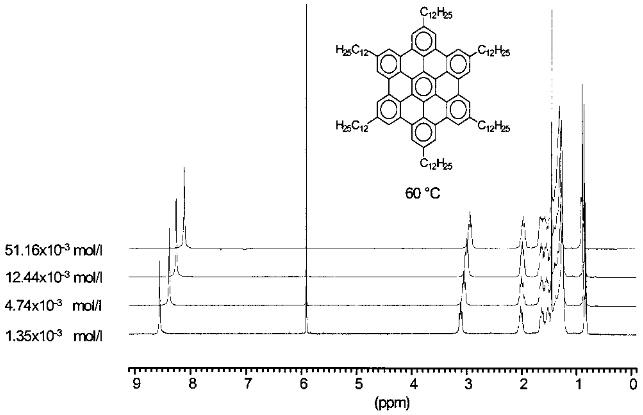

Figure 6. Concentration-dependent ^{1}H NMR spectra of **22** ($R_{1-6} = C_{12}H_{25}$) at 60 °C.

In a similar approach, the aggregation of phenylacetylene macrocycles **65** (Chart 1) in solution have been studied with ^{1}H NMR spectroscopy.[169,170] They have determined the association constant for dimerization, K_{assoc}, by curve fitting the concentration dependence of the proton chemical shift to a model for monomer−dimer equilibrium. The results obtained from NMR studies, e.g., aggregation constants and aggregate size, have independently been verified by vapor pressure osmometry experiments. Further, it has been well documented in the literature that aryl groups tend to associate in either a face-to-face or an edge-to-face orientation.[175,176] In the phenylacetylene macrocyclic systems **65**, it was possible to assign a face-to-face π-stacking arrangement to the macrocycles in solution.[169,170] However, the nature of the forces that cause these self-association phenomena are still not totally clarified, quadrupole–quadrupole and/or van der Waals interactions are being discussed in the literature.[177,178] These aromatic $\pi-\pi$-interactions are suppressed when the periphery of the macrocycle is substituted with bulky *tert*-butyl groups which prevent the molecules from approaching each other.[172,179]

Solid-state NMR is an important tool for investigating aromatic packing behaviors.[156,157,179,180] Using these techniques, the bulk properties and the solid-state characteristics of a material can be studied. In the case of the alkyl-substituted HBC derivative **22** ($R = n\text{-}C_{12}H_{25}$),[155] extreme high-field shifts of $\delta = 5.6$ ppm have been recorded[156] for the aromatic protons in the solid-state phase indicative of the pronounced intermolecular deshielding interaction present in the bulk. Fast magic-angle spinning (MAS) and double-quantum ^{1}H solid-state NMR spectroscopy have been used to further investigate the $\pi-\pi$-packing in the columnar structures formed by hexabenzocoronenes and triphenylenes.[179] In the crystalline phase of the former **22** ($R = n\text{-}C_{12}H_{25}$), three distinct aromatic signals are found in the single-quantum MAS spectrum, despite the hexagonal molecular symmetry.[156] These three distinguishable peaks are explained in terms of different ring-current influences of adjacent layers which the aromatic core protons experience since they are stacked in a columnar–rectangular herringbone-type fashion. These observations are in agreement with the crystal structures obtained from substituted[179,181] and unsubstituted[182] HBCs. However, upon increasing the temperature so that the liquid crystalline phase is entered, the three aromatic signals merge into a single resonance. This can be attributed to the transformation into the columnar hexagonal mesophase and fast axial motion of the HBC disks around the columnar axis.

Quantum chemical ab initio calculations are in agreement with the solution and solid-state experimental data presented above.[173,174] The theoretical proton resonance frequency of an isolated HBC **22** (R = H) disk was calculated to be $\delta = 9.3$ ppm. Computation of a trimeric aggregate system also revealed three different high-field ^{1}H NMR signals for the aromatic core, as experimentally found with solid-state NMR techniques.[156,173,174]

The extreme downfield shifts of, e.g., $\delta = 9.5$ ppm for compound **66**[183,184] nicely document the diatropic character of the PAHs. These chemical shifts originate from a complex interplay of ring size, perimeter type, and aggregation. Not surprisingly, the protons inside the ‘cove-type’ region, protons H_a (see compounds **67**, **68**),[184] experience a more pronounced downfield shift, resulting from the deshielding effect of the five neighboring benzene rings, than those in the bay regions. As already mentioned above, aggregate formation with a partial face-to-face arrangement of the disks leads to an increasing upfield shift of the proton NMR signals.

An important consequence of the hexagonal symmetry of HBC **22** is the occurrence of energetically degenerate orbitals, which should lead to the formation of high-spin states upon electron-transfer reactions.[185] Indeed, hexa-substituted benzene derivatives as well as triphenylenes[186−188] and coronenes[189,190] have been important subjects of dianion and dication formation. Triplet ground states have been found for the dianions and dications of triphenylene.[186−188] On the other hand, coronene displays only thermally excited dianions and dications, possibly a consequence of Jahn–Teller distortions.[189,190] Not surprisingly in view of the larger size, an extended redox sequence can be established when subjecting alkyl-substituted HBC **22** ($R = n\text{-}C_{12}H_{25}$) to alkali-metal reduction. This sequence ranges from the mono- to the tetraanion, and the ions can be fully characterized by ESR and UV–vis spectroscopy. If one records the ESR spectrum of the dianion in a frozen matrix, one clearly detects a zero-field splitting which provides evidence in favor of a triplet structure. Temperature-dependent measurements, however, leave no doubt that the ground state is a singlet. Interestingly, a $m_I = {}^3/_2$ state can be detected for the trianion, which, in accordance with MO calculations, suggests the existence of at least three energetically degenerate LUMO levels.

The electronic absorption spectra of PAHs have attracted great attention whereby different approaches toward classification of the particular bands have been proposed.[142] A generally valid approach[191] identifies (i) α-bands (L_b in the Platt nomenclature[192]) which relate to the longest wavelength absorption of benzene and are relatively weak and possess a distinct vibrational structure, (ii) p-bands (L_a) of medium intensity and are more sensitive to a linear annulation than the α-bands, and (iii) β-bands (B_a, B_b) which are intense and have no vibrational structure.

The characterization of large PAHs by UV–vis spectroscopy is not straightforward in view of the insolubility of higher homologues in organic solvents. In this case, one has referred to transmission measurements for thin films using various deposition techniques. A number of techniques can be used for the preparation of thin film samples. In the field of special coatings, the following are of interest: (a) direct ion beam deposition, (b) sublimation, (c) vacuum graphite arc sputtering on aluminum plates, (d) laser vaporization, (e) spin-coating, and (f) solution-casting. For the larger PBAHs, solid materials were “smeared” onto quartz plates to obtain amorphous films of sufficient quality, and since in a number of cases alkyl-substituted analogues with residual solubility are available, solid-state and solution UV–vis spectra can be compared, and this is shown for a typical example in Figure 7.[193] The presence of organic radicals in the crude PBAHs are indicated by an atypical, very broad absorption in the NIR range

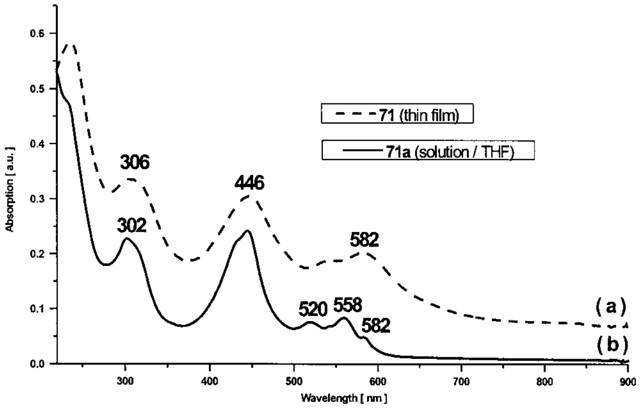

Figure 7. Comparison of solution and solid-state UV−vis spectra of a large PBAH with alkyl substituents (**71a**) and without (**71**).

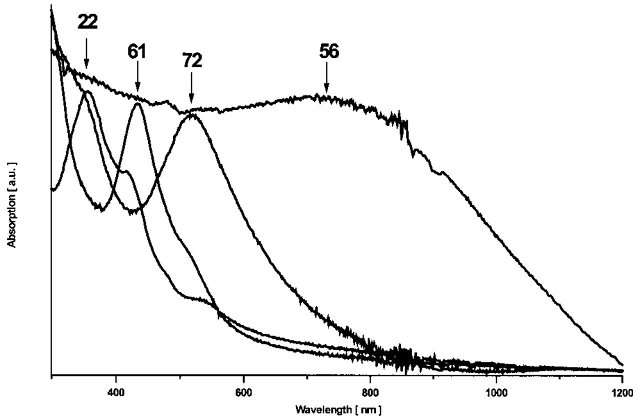

Figure 8. Solid-state UV−vis spectra of homologous series of PBAHs with hexagonal symmetry (D_{6h} symmetry).

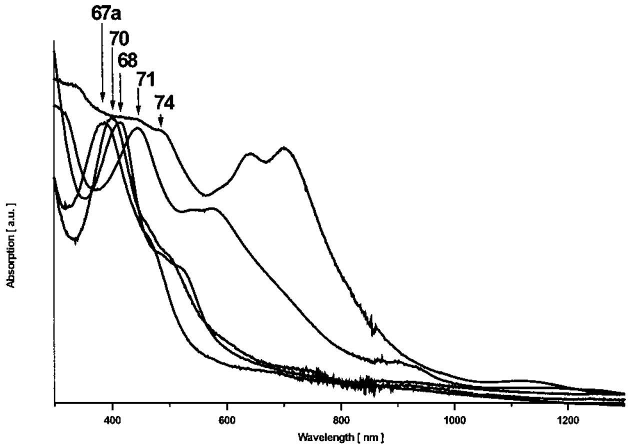

Figure 9. Solid-state UV−vis spectra of homologous series of PBAHs with "linear" annulation (D_{2h} symmetry).

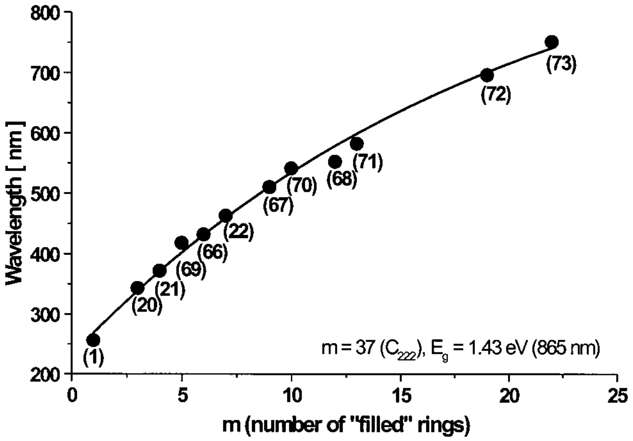

Figure 10. Correlation of α-band absorptions of PBAHs versus the number of "full" rings (m), extrapolated to $m = 25$ (compound **73**).

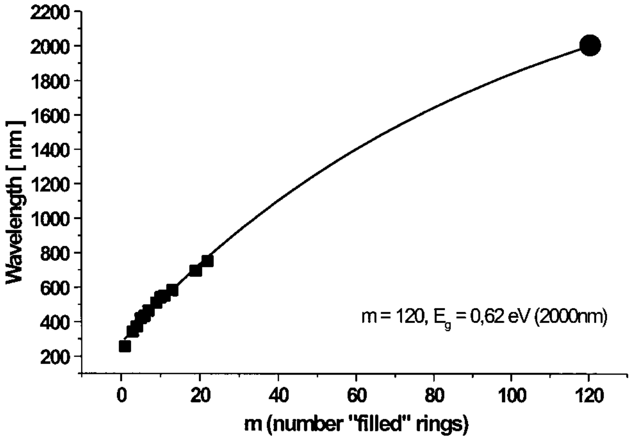

Figure 11. Correlation of α-band absorptions of PBAHs versus the number of "full" rings (m), extrapolated to include PBAHs with $m > 120$.

(900−1500 nm) and confirmed by EPR spectra ($g = 2.00023$). It is possible that radical cations are formed during the oxidative conditions of the final synthetic step. These species could be eliminated by reduction of the crude PBAH samples with hydrazine. The UV−vis spectra of thin films are similar to the corresponding solution spectra of the substituted analogous compounds, although the optical absorption bands are broader and weakly red shifted (by a few nm). Some typical solid-state spectra are reproduced in Figures 8 and 9. Compounds included in this study[193] include **20**−**22**, **56**, **61**, and **67**−**74**. Generally the spectra are progressively shifted and the different bands, α, *β*, and para, retain their characteristic features only the intensity is different. A characteristic feature of both solution and film spectra is the occurrence of aggregation bands which can make the identification of specific transitions difficult. A detailed discussion of the spectral features is, of course, beyond the scope of this text. The correlation of the α-band absorptions of the PBAHs investigated in this study vs number of "full" rings gives a straight line as in Figures 10 and 11. This extrapolation is strictly limited to the all-benzenoid PBAHs and leads to a value of 865 nm (1.43 eV) for the largest compound **56** and to a maxima value $\lambda_{\alpha}(\max) = 2000$ nm (0.62 eV) for polycyclic benzenoid aromatic hydrocarbons with $m > 120$ aromatic rings. Energy gaps could be calculated from these α bands and were seen to decrease with increasing size. A specific point which should be emphasized here follows: As a result of the new synthetic routes, molecularly defined graphite-related PBAHs are obtained which can be processed in the gas phase or by deposition from solution and which upon appropriate alkyl substitution are even meltable (see below). Thus, thin films are obtained possessing broad absorption bands covering the hole spectrum of visible light which qualifies such graphitic materials, e.g., for photovoltaic experiments.[194]

Chart 1

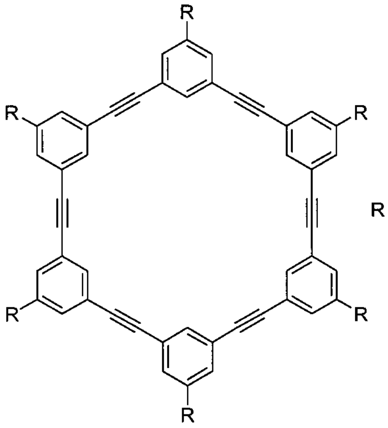

R = *e.g.* alkoxy, *t*-butyl

65

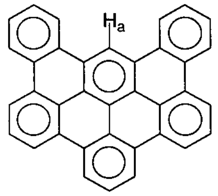

66

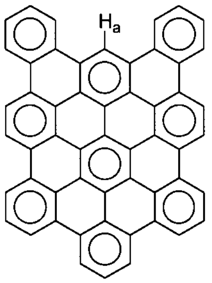

67

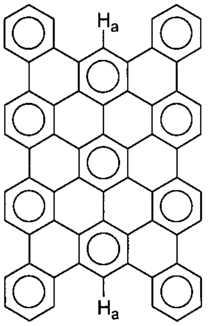

68

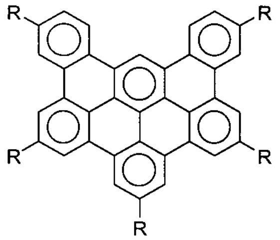

R = H **66**
R = n-alkyl **66a**

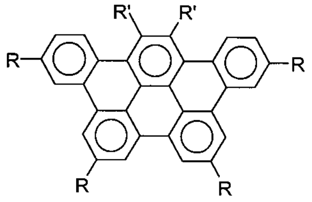

R, R' = H **69**
R, R' = n-alkyl **69a**

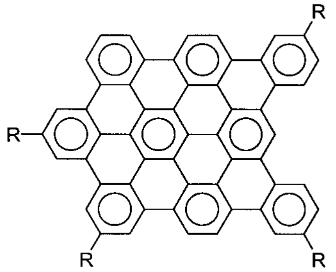

R = H **67**
R = n-alkyl **67a**

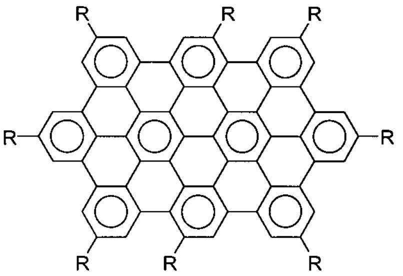

R = H **70**
R = n-alkyl **70a**

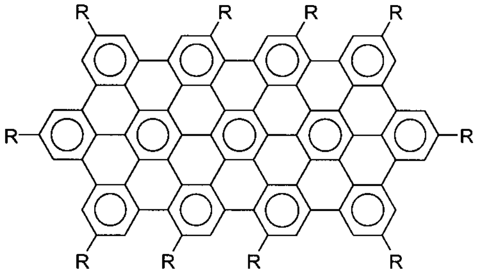

R = H **71**
R = n-alkyl **71a**

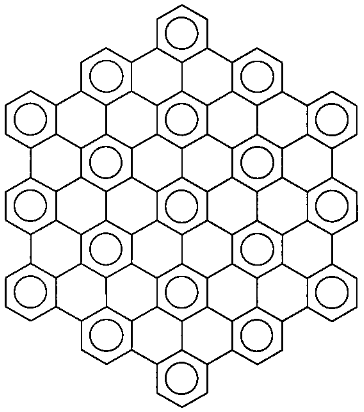

72

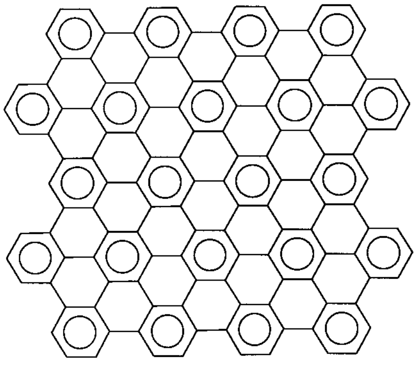

73

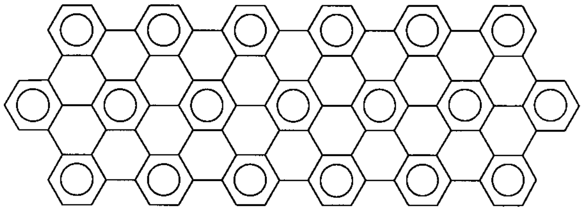

74

In relation to these solid-state measurements, a detailed study,[195] both empirical and theoretical, of the effect of disorder on the electronic excited states of a hexa(alkylthio)triphenylene **20** (R = *S*-alkyl) in the bulk state has been conducted. Small but measurable shifts in the absorption maximum are seen which correspond perfectly with the phase transitions of this PBAH, emphasizing the importance of the state of matter in which compounds are studied. From these measurements together with theoretical treatments, estimations of the number of interacting chromophores could be estimated.

C. Crystallographic Characterization

X-ray characterization of PAHs provides valuable information in three different areas: (1) measurement of bond lengths and angles can support theories concerning aromaticity; (2) the question of planarity of a particular PAH, at least in the solid state, can be unambiguously answered; (3) orientation within crystals (morphology) gives insight into the prevalence of specific interactions as well as explaining physical phenomena.

Regarding the first issue, X-ray measurements have been instrumental in providing structural proof of the concepts of aromaticity. The reader may look in the literature compilations[182,196] of existing X-ray structures for a broad range of types of PAHs, although the number certainly does not reflect the number of compounds prepared to date. Perhaps the greatest limiting factor is the prerequisite for suitable single crystals.

A particular case where X-ray has been very successful is in validating Clar's theory[143,197] in the case of PBAHs. Should a structure consist of alternating six-membered rings which are either benzenoid or "empty", the bond lengths determined from X-ray should reflect this. From the bond lengths, bond orders may be calculated which reflect the degree of single- or double-bond character. This can clearly be seen in the case of the smallest PBAH, triphenylene **20** (R = H).[198] Significant bond-length alternation is seen in the central (empty) ring while much less is seen in the outer (full) rings. Unfortunately, the number of crystal structures which exist for PBAHs is even more severely limited compared to PAHs in general. It is surprising that with recent advances in crystallization techniques for PAHs that more of these structures have not been elucidated. Examples include a number of persubstituted triphenylene derivatives **75**−**79**,[199−202] dibenzo[*fg*,*ij*]phenanthro[9,10,1,2,3-*pqrst*]pentaphene (**66**),[183] phenyldibenzo[*fg*,*ij*]phenanthro [9,10,1,2,3-*pqrst*]pentaphene (**80**),[183] 9,18-diphenyltetrabenz[*a*,*c*,*h*,*j*]anthracene (**81**),[183] hexabenzotriphenylene **82**,[88,203,204] HBC **22**,[182,205] and an alkyl derivative of HBC **83**.[181] In all these cases, the all-Clar structures could be supported from the bond lengths.

A further question which may be answered by X-ray is that of planarity. Recent papers[206,207] disclose that of the thousands of possible PAHs with 10 rings, the vast majority should be nonplanar, even chiral, structures resulting from steric factors. Highly notable examples of nonplanar PAHs include helicenes, fullerenes, bowl-shaped components of fullerenes, and nanotubes.[206,207] Several intriguing species have been prepared in which the rings are forced out of planarity due to intramolecular steric interaction between substituents. These interactions become important when the angles by which substituents protrude from the sp^2 periphery are such that they would approach adjacent substituents closer than allowed by van der Waals radii.

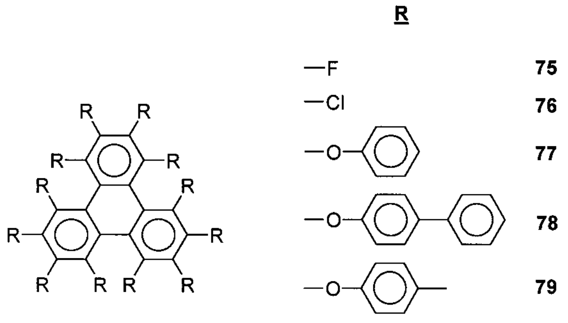

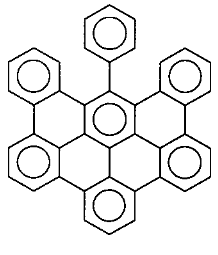

80

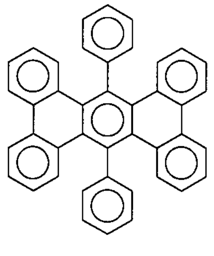

81

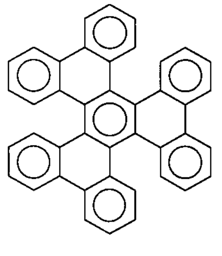

82

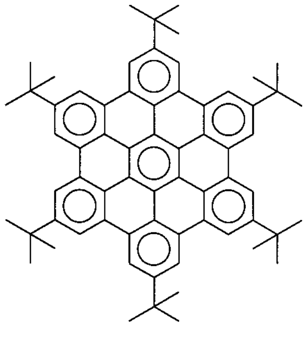

83

Dramatic deviation from planarity may be induced upon replacing the peripheral hydrogens of an otherwise planar PAH with larger substituents. A simple case is perchlorocoronene **84**.[202,208] Interaction of the chloro atoms is not severe due to the zigzag periphery of the coronene core. This effect could easily be visualized by considering the coronene core as a circle and considering the angle between the C−Cl bond as a tangent to this circle. This angle is much less acute than might be seen with an armchair periphery. Steric interaction between the chlorine atoms is sufficiently relieved by torquing the 12 peripheral carbons out of plane (by ~0.3 Å) while the 12 central carbon atoms remain essentially coplanar. Analysis of the bond lengths confirmed the view that perchlorination does not significantly affect the bond orders. The radiation resistance of this compound has allowed its visualization in an epitaxial film at 1 Å resolution by a special technique.[208] More pronounced nonplanarity is observed after replacing the chlorides

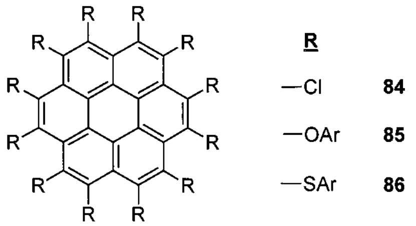

with more bulky aryloxy **85** or arylthioether groups **86**, compounds which have implications as inclusion compounds due to their shape.[202,209] It is interesting to note that the thioether compounds are isolated as red or purple crystals as opposed to yellow coronene and its chloro and aryloxy derivatives.

Returning to Clar PBAHs with armchair peripheries, a number of examples of nonplanar triphenylene derivatives have been published.[199−202] Even the very small fluorine atoms (compare van der Waals radii H = 1.1 Å, F = 1.35 Å) of perfluorotriphenylene **75**[201] are sufficiently large to cause nonplanarity. Much more drastic effects are seen in perchlorotriphenylene **76**[199−202] (van der Waals radius Cl = 1.75 Å) with C_2 symmetry similar to the perfluoro derivative but where distortions of the central ring are the greatest known for any triphenylene. Although the molecule is quite stable, this extreme bending makes it a target for electrophilic attack, producing a carbenium ion which rearranges to a much less strained spiro compound. Interestingly, perchlorination results in a change in optical properties (golden yellow crystals compared to colorless triphenylene and peraryloxy derivatives**)**. Peraryloxy derivatives have also been prepared with the aim of investigating crystalline inclusion compounds. In one such example, compound **79**,[201] it was shown that the torque induced in the triphenylene core is greater than in the perfluoro **75**[201] but smaller than in the perchloro derivative **76**.[199−202]

Very few examples of crystal structure determinations for larger nonplanar PBAHs exist. These can be considered as a series of compounds related to the fully planar HBC. Deviations range from nearly planar to markedly nonplanar as single bonds comprising the “empty” rings or the full rings themselves are removed from the structure of HBC. For the former series, three different highly nonplanar geometries are obtained by removing two, three, and four “single” bonds to yield phenyldibenzo[*fg,ij*]phenanthro[9,10,1,2,3-*pqrst*]pentaphene **80**,[183] hexabenzotriphenylene **82**,[88,203,204] and 9,18-diphenyltetrabenz[*a,c,h,j*]anthracene **81**,[183] respectively.

Removal of one of the “full” benzene rings (plus two empty rings) of HBC produces dibenzo[*fg,ij*]phenanthro[9,10,1,2,3-*pqrst*]pentaphene **66**,[183] which contains a “double bay” region. This structural feature might be expected to slightly perturb the planarity. However, X-ray analysis shows that the molecule is nearly planar, with the largest deviation of any single carbon atom from the calculated best plane of 0.06 Å.

Recently, a highly nonplanar HBC **58**[163] has been prepared with 18 methoxy groups in the periphery. The outermost benzene rings alternate in up−down fashion, producing a “saw-tooth” periphery much like that seen in perchlorocoronene. As noted in the triphenylene and coronene cases, peretherification makes little difference in the optical properties compared to the parent compounds.

Nonplanarity in the bulk state may even be induced by *intermolecular* steric interactions as seen in the case of HBC containing six bulky *tert*-butyl groups **83** on the periphery.[181] The nonplanarity is not substantial but still it exists in the single crystal (largest deviation of the quaternary carbons of the *tert*-butyl groups from the plane of the HBC core is 0.56 Å.)

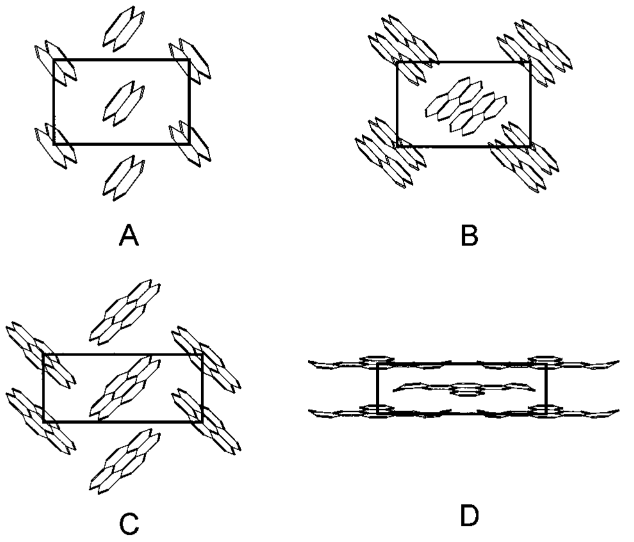

Figure 12. Classification of different crystal morphologies for PAHs: (A) herringbone, (B) sandwich−herringbone, (C) γ-structure, (D) β-structure.[196]

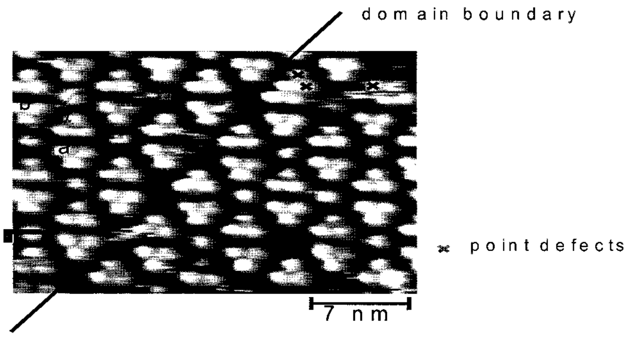

Figure 13. STM image of **22** (R_1 = Br, R_{1-5} = $C_{12}H_{25}$).[158]

Another important issue which is addressed by X-ray is that of crystal structure, as opposed to molecular structure. The way in which the molecules order in the solid state gives valuable information about the relative importance of specific interactions, molecular shape, and size, which are important for future rational design of molecular materials as well explaining bulk phenomena including mechanical, optical, and electrical properties. Desiraju and Gavezzotti compared the crystal data for 32 PAHs in order to develop a predictive scheme based on molecular characteristics.[196] They divided crystal morphologies of PAHs into four main classes as shown in Figure 12. While their scheme proved highly useful for correlation, it has been shown in at least one case, benzo[1,2,3-*bc*:4,5,6-*b′c′*]dicoronene,[210] to be ineffective for prediction. Alkyl-substituted HBCs fit well into the predictive scheme. While HBC **22** crystallizes in the γ morphology,[210] the hexa-*tert*-butyl derivative **83**[181] gives sandwich−herringbone, a consequence of increasing the number of atoms which contribute to glide (periphery) relative to stack (large aromatic core), in the nomenclature of Desiraju and Gavezzotti.[196]

Herringbone and sandwich–herringbone lattices are in most cases preferred over a true columnar packing. A remarkable case of a columnar arrangement in single crystals is obtained upon electrocrystallization of small polycyclic aromatic hydrocarbons, such as pyrene and fluoranthene. While stoichiometries can vary, an A_2X stoichiometry (A = PAH, X = counteranion) is most common, pointing toward only a partial oxidation of the π-system. The resulting columnar structure is made from face-to-face arranged π-systems, while electroneutrality is achieved by the separate stacks of counterions. The occurrence of the mixed-valence states and of an extended channel for charge transport provides the structural basis for the electrical conductivity of the radical cation salts.

The potential applications of PAHs have also initiated the exploration of organometallic hydrocarbon complexes as possible candidates for stabilizing aromatic polyenes, increasing conductivity, and inducing ferromagnetism. In the past 10–15 years, a variety of different transition-metal complexes with a number of large PAHs has been synthesized.[211–220] These complexes have a strong influence on the structure, reactivity, and aggregation behavior of their aromatic partners through overlap of the ring π- and π^*-orbitals with the appropriate orbitals of the metal atoms. As to the cause of these contributions, one important question has been posed: Do transition metals reduce the aromaticity of benzene?[221]

A (triphenylene)$Cr(CO)_3$ complex and its crystal structure[212] has been described in which the Cr–C distance of this η^6-complex is around 2.2 Å, common for transition-metal–carbon bond distances. A redox-tunable near-IR dye based on a trinuclear ruthenium(II) complex of hexahydroxytriphenylene **87** has been prepared.[220] Here, the absorption maximum of the triphenylene–$Ru(II)_3$ complex may be tuned in steps according to the oxidation state (degree of quinoidal character).[220] Organosilver(I) complexes of 9,10-diphenylanthracene, rubene, benzo[*a*]pyrene, and coronene have been prepared and investgated crystallographically.[219] Starting from the different monomers, complexation with silver(I) perchlorate afforded four topologically different structures. Characterization of the 9,10-diphenylanthracene complex revealed a discrete monomeric structure, whereas the X-ray analysis of the silver(I) complex with rubene showed a 3D polymeric structure.[219] A double-helical formation was observed for the structure formed with benzo[*a*]pyrene and a triple-decker polymeric structure for coronene.[219]

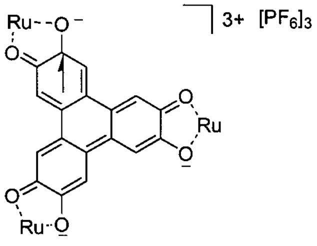

87

A mono- and a bis-tricarbonylchromium complex of a hexabenzocoronene derivative substituted with six *tert*-butyl groups **83** has been prepared.[181] Both the mono- and the bis-chromium complex were formed in the reaction but could be separated using column chromatography.[181] The ^1H and the ^{13}C NMR spectra do not show any unusual shifts to high fields of the aromatic proton signal. A single-crystal X-ray structure obtained from the first revealed a double-herringbone packing behavior whereby the arrangement of the aromatic disks is dominated by the formation of dimers (in which the $Cr(CO)_3$ ligands point in opposite directions and are located with maximal distance on the disks) in the crystal lattice.[181]

D. Packing Phenomena and Supramolecular Architectures

Substituted and unsubstituted PBAHs can be made to self-assemble in 2 and 3 dimensions as a result of intermolecular interactions and interactions with surfaces or templates. Self-assembled monolayers may be deposited on a variety of surfaces to yield, in essence, 2-dimensional crystals.[155,158,222–227] The electron-rich cores are particularly amenable to visualization by scanning tunneling microscopy (STM), giving bright spots which provide a clear map of the 2D lattice.[223] The fruits of these endeavors include characterization of the molecule which the chemist desires, insight into packing behavior as the physicist desires, and also development and greater understanding of the method as the analyst desires.

The high thermal stability of large unsubstituted PBAHs such as **88**[46,228] permits fractional sublimation at 550–650 °C under ultrahigh vacuum conditions.

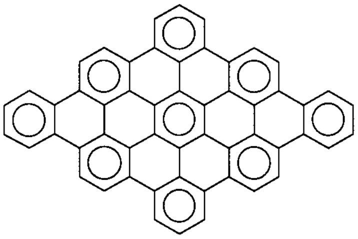

88

The self-organization of the sublimed molecules leads to epitaxial growth of monomolecular adsorption layers on substrates such as molybdenum sulfide and HOPG. Using desorption spectroscopy it was even possible to determine the binding energy of the molecule to the surface.[46,228] HBC **22** forms a hexagonal lattice, indicated by earlier low-energy electron diffraction (LEED) measurements and later confirmed by STM.[229,230] Furthermore, submolecular resolution can be observed in the STM images of these PBAHs, as will be discussed in section V.

The coincidence of substrate and adsorbate symmetries is crucial for the ordering, i.e., for the formation of 2D crystals. Additionally, the HBC **22** molecule, which itself resembles a graphite segment, is oriented along the HOPG lattice in the same way as an (second) imposed graphite layer.[230] This concludes that the substrate rules the orientation of the molecules. Ordered monolayers of HBC could also be used as a ground floor for deposition of a second layer of a perylenetetracarboxylic dianhydride **89**.[230] This resulted in true organic–organic heterostructures with interfaces flat on a molecular level, presenting the first example of ordered growth of layers (from two different planar molecules) in a heteroepitaxially stacked film.[230]

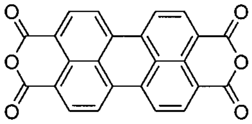
89

When the PBAHs are substituted with flexible alkyl chains they can be deposited on the surface by physisorbtion from solution.[155,161] STM images obtained at the solid–liquid interface exhibit lower resolution due to a constant equilibration between adsorbate molecules and molecules in solution as well as conformational mobilities faster than the STM scanning rate. Visualization by STM offers support to conclusions which might be drawn from 3D measurements (X-ray) such as interdigitation of side chains, interaction of heteroatoms, hydrogen bonding, etc.[231] Here, regularly ordered monolayers are formed, where the flexible alkyl chains fill the space between the aromatic cores. In the case of HBC **22** (R = $C_{12}H_{25}$), two coexisting packing patterns were observed: one rhombic lattice and one where dimers oriented in parallel rows.[230] "Surface-induced chirality" was noted[223] in monolayers of nonchiral triphenylenes **20** (R = alkoxy) on the nonchiral surface HOPG. The disks were ordered in a 2D hexagonal array as in the 3D mesophase, although with smaller intermolecular distances. The appearance of a superlattice in derivatives with longer alkyl chains, as evidenced by differing contrasts, was attributed to "chiral domains".

As mentioned above, incorporation of heteroatoms can have strong influences on the two- and three-dimensional crystal packing of PAHs.[232–234] Recently, the synthesis and the STM characterization of a bromo-functionalized HBC derivative **22** (R_1 = Br, R_{2-6} = alkyl) has been reported.[158] In this case, trimeric assemblies and single molecules are arranged in a symmetric two-dimensional crystal, in which single molecules in the center are surrounded by six trimers and every trimer is surrounded by three single molecules (Figure 12). The formation of trimers is attributed to attractive interactions between the bromine atoms of neighboring molecules. Assuming a triangular arrangement where the bromine atoms point toward the center, the distance of the aromatic cores is estimated to be 1.64 nm. This is in agreement with the experimental value of 1.6 ± 0.1 nm. However, one cannot make a final conclusion about the origin of the interactions due to the considerable error margin of the calculations. Furthermore, it was attempted to observe other intermolecular interactions such as hydrogen bonds which are likely to be present in the case of the amino-functionalized HBC **22** (R_1 = NH–alkyl, R_{2-6} = alkyl);[158] the STM image reveals rows of dimers. Experimental data, however, show that the distance between the amino groups of neighboring molecules is presumably too large for intermolecular hydrogen bonding. Taking into account that the given data for the unit cell has a reasonably large error margin, hydrogen bonds could not completely be excluded.

Not surprisingly, large PAHs are known to have very high melting points. When carrying a number of alkyl-, alkoxy-, or alkoxycarbonyl substituents, the PAHs melt at relatively low temperatures. Melts of these compounds are not isotropic but instead give rise to liquid crystalline phases, a consequence of combining the rigid cores with liquidlike periphery.[33,235] The ordering can of course be related to the mesomorphic properties of pitch which contains a broad range of such persistent PAHs.[34,236] In fact, even the unsubstituted PAHs HBC and benzo[1,2,3-*bc*:4,5,6-*b′c′*]dicoronene have been carbonized to produce highly anisotropic cokes.[34,236] Polarization microscopy, differential scanning calorimetry, and X-ray-diffractometry are used to characterize such phases. Hexasubstituted triphenylenes **20**,[237] octasubstituted dibenzopyrenes **21**,[238,239] and hexasubstituted hexabenzocoronenes **22**[155,157,158] form discotic mesophases with columnar arrangements of face-to-face positioned disks and, in some cases, even a hexagonal superstructure of the columns. It should be noted that these mesophases are dynamic. Thus, uniaxial rotation of the disks and even exchange of the disks between columns can occur.

Nevertheless, the resulting order in the stacked crystalline phases or columnar liquid crystalline phases are of great importance because they give rise to channels for charge-carrier transport,[194,240–248] e.g., in photoconduction experiments. The significance of the supramolecular order for a photoconduction process as being relevant, e.g., for electrophotography, is obvious. One would want to increase the photocurrent, but the concentration of charge carriers is limited. Consequently, it appears straightforward to increase the charge-carrier mobility, and this can be achieved by increasing supramolecular order. It appears, again, that a materials property, such as photoconductivity, can only be described when supramolecular and even morphological aspects are included. In order for such a design to become practical, however, further requirements must be met, because the columns have to span the gap between electrodes instead of lying down on the surface of the electrodes. Anisotropic melts are not the only way of achieving supramolecular $\pi-\pi$-stacking; the columns can be mechanically aligned by shearing forces. The melts can be extruded into thin fibers, which after cooling appear from 2D X-ray diffractometry as possessing, again, a columnar arrangement with the stacking axis along the fiber axis.[158] While we will not further consider the aspects of processing, the molecular design deserves further comment.

In the case of triphenylenes, two exceptional examples of altered order in the liquid crystalline state are reported for alkoxy-substituted monomeric species with shorter alkyl chains **20** (R = –*O*-butyl) and dimeric molecules **90**[249–252] linked by flexible alkanediyl spacers and thioether-functionalized monomers. In the former, a more rigid "plastic liquid crystalline" phase is observed with decreased interdisk spacing and restricted lateral and longitudinal freedom. For hexakis(hexylthio)triphenylene **20** (R = *S*-hexyl), in addition to the normal hexagonal discotic phase, a helical discotic phase is observed with long-range ordered columns consisting of at least 220 molecules.[253] More bulky substituents in the periphery can induce higher order by inhibiting molecular motions which decrease order, as discussed earlier for the HBC compound with *p*-alkyl-phenyl groups **60**.[157]

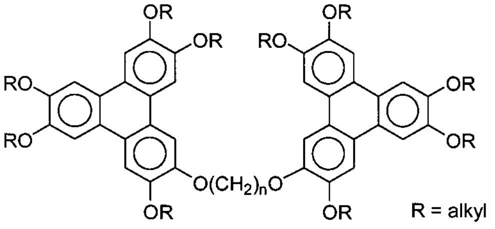

90

Order may also be enhanced by incorporating, in addition to π–π-stacking, structure forming principles such as hydrogen bonding, ionic or covalent interactions, and interaction with templates.[254–263] It has been suggested that mesophases formed from polyelectrolyte–surfactant complexes have smaller domain boundaries than those seen in mesophases of surfactants alone based on the reduction or absence of sharp dislocations in the optical textures of the former.[264,265] This principle was exploited in preparing the polyelectrolyte complex **92**[266,267] from the acid-functionalized HBC **91**.[268] X-ray measurements reveal high local order (effective π–π-overlap) as well as remarkable long-range order. Further, visualization of thin cross sections by electron microscopy revealed striped features which are ascribed to microsegregation of the columns from the polysiloxane matrix. These patterns are free of dislocations and suggest column lengths of at least 200 nm.

In related 2-dimensional cases, stacking may be ordered by interaction at the air–water interface as in Langmuir and Langmuir–Blodgett techniques[254] or at the liquid–solid interface as with thiol-functionalized disks covalently bound to gold surfaces. In the former, surface active molecules, e.g., PAHs containing hydrophilic groups, are spread on a well-defined template (water) and compressed to highly ordered monolayers which may then be deposited on solid substrates. This technique has been extensively utilized to study amphiphilic triphenylenes.[254–259,269] In the monolayers, the disks are generally aligned normal to the surface in 2-dimensional columns oriented more or less in the deposition direction. Some important observations include thermal transitions corresponding to those observed in the bulk state,[259,270] insertion of electron acceptors into the columns and their charge-transfer complexes with increased order,[256–258,269] and time-resolved photocurrents after photoexcitation.[255] Similarly, X-ray measurements of monolayers formed from the acid-functionalized HBC **91** revealed two phases dominated by either π-stacking or alkyl side chain ordering, depending on the applied pressure.[271] Kelvin force microscopy was employed to demonstrate a significant difference in electronic properties of these two phases. In the related case of self-assembled monolayers of thiol-functionalized triphenylenes on gold surfaces,[260–263] the disks can be ordered edge-on or face-on depending on the number of thiol functions included. Columns of edge-on disks with lengths greater than 100 nm were observed by AFM,[260] and upon inclusion of trinitrofluorenone, clearer STM images were obtained,[263] and increased overall order and persistence length of the columns[261] were observed.

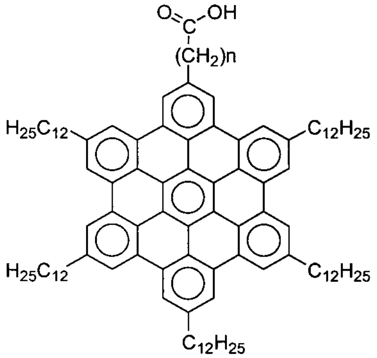

91

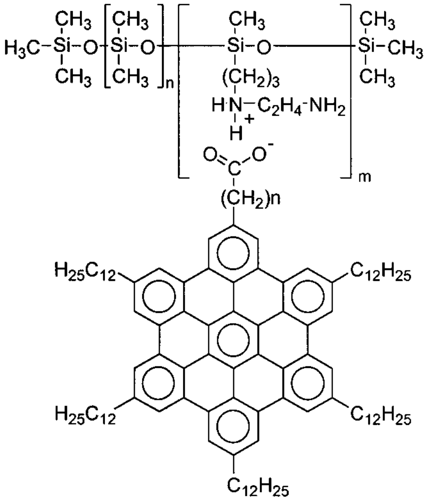

92

In considering the bulk electrical properties of pure PAHs, it is interesting to first traverse from the measurements which can be made on single molecules, to small ensembles, to the bulk material. In the case of hexaalkyl HBC **22** (R = $nC_{12}H_{25}$), diode-like current–voltage curves are observed for the cores of single molecules using scanning tunneling spectroscopy (see section V).[155] Proceeding to small ensembles or to the bulk, one must consider the possibility of the molecules acting as nanowires where transport processes occur strictly intermolecularly through the overlapping π-systems as opposed to the situation of conducting polymers.[194] These channels of π-systems are coaxially insulated by the substituents attached to the periphery of the aromatic core, thus the designation of nanowires. Transport processes in discotic liquid crystals have been studied extensively in recent years.[194,240,241,243−248,272] A recent paper summarizes some the important concepts of this situation including considerations of band gaps of such ensembles and charge injection.[194] Mechanisms for charge transport in the triphenylene dimer **90**[244] have been proposed after combining pulse radiolysis time-resolved microwave conductivity (PR-TRMC) measurements and time-of-flight (TOF) experimental techniques as well as simulations.[248] PR-TRMC utilizes a rapidly oscillating electric field to probe charge-carrier motion without the need for electrodes, as required in the case of TOF measurements.

Charge-carrier mobilities measured for triphenylenes **20** and HBC **22** are seen to be much higher in the crystalline phase.[241,244−246,248] Mobilities in the crystalline phases of some triphenylenes are more sensitive to temperature changes, which is attributed to the smaller $\pi-\pi$-overlap creating greater susceptibility of the stacks to perturbation by the side chains. The drop in charge-carrier mobility for both systems upon entering the mesophase is ascribed to a decrease in order. In the case of substituted HBCs, both crystal structure and solid-state NMR measurements indicate that in the crystalline form, the disks are stacked with an overlap much like that in graphite giving optimum $\pi-\pi$-overlap. Further, HBC **22** is three times the size of triphenylene, and this gives rise to much more stable mesophases, i.e., the temperature range between melting and isotropization is much broader, and, more importantly, the charge-carrier mobility in the mesophase is much higher, which can readily be ascribed to the increasing number of $\pi-\pi$-contacts.

The message to be drawn from these few examples is that π-conjugation and charge-transport processes cannot be restricted to a molecular description but include intermolecular effects comprising order at various lengths scales. This order may be controlled by mechanical processing, direction of the molecular design by intelligent liquid crystal engineering, and incorporation of additional structure forming principles such as templates.

E. “Superbenzene” Chemistry

Consideration of the molecular structure of HBC **22** (see section III.1), with its hexagonal symmetry, suggests its description as a “superbenzene”, where each peripheral benzene ring is equal to one sp^2-carbon of benzene.[273] In this fashion, one includes the well-known nomenclature for substitution patterns for benzene such as *ortho*, *meta*, and *para* (This scheme becomes more complicated when substituents are placed in the bay positions). Further, transition-metal-catalyzed coupling/substitution reactions[158] provide superbenzenes with electron-withdrawing (ester, cyano) and -donating (alkoxy, amino) groups whose effects on the electronics of the core can be delineated in the near future, as continuously pursued for benzene over the years. In particular, scanning tunneling spectroscopy can be used to investigate the effect of these groups on the current−voltage response as mentioned previously for all-alkyl-substituted superbenzene **22** (R = alkyl).[155]

From this viewpoint, the role of superbenzene as a repeat unit of giant fused PAHs is analogous to using benzene as a building block to produce fused homologues. This is clear in the naming of the supernaphthalene **63**,[160] superphenalene **93**,[160] and supertriphenylene **64**,[160] in which two, three, and four superbenzenes are fused, respectively.

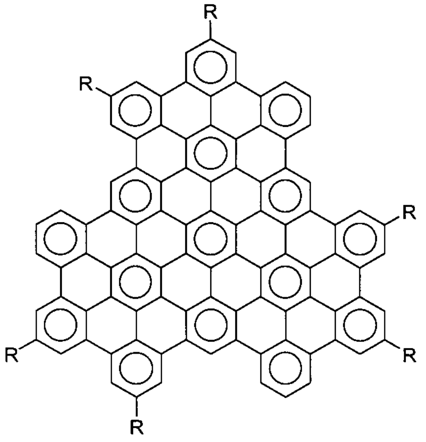

R = H, R = *t*-Bu

93

Functionalization of superbenzene permits covalent linking leading to, e.g., superbiphenyl **94**[225] and the supertolane **95**,[225] prepared by transition-metal-catalyzed coupling reactions starting from the monobromo derivatives. Superbenzene as a building block of more complex macromolecular architectures becomes particularly obvious from the fact that a benzene-like chemistry originates from the synthesis of mono-, *o*-di-, and *p*-disubstituted species mentioned above. Keeping in mind the versatile role of functionalized benzene derivatives in polymerization and polycondensation chemistry, it now becomes possible to design an analogous chemistry of superbenzene. Through natural progression from the superbiphenyl, *p*-difunctionalized HBCs can be incorporated into the main-chain polymer **96**[274] analogous to substituted polyphenylenes. Contrary to the latter, **96** is an intractable material despite the solubilizing substit-

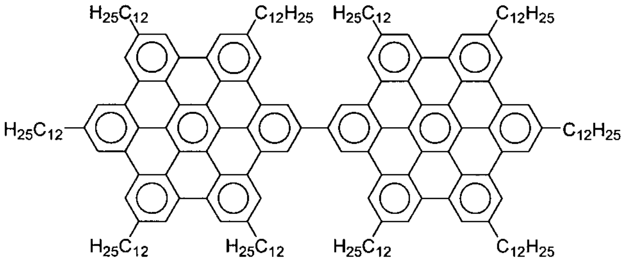

94

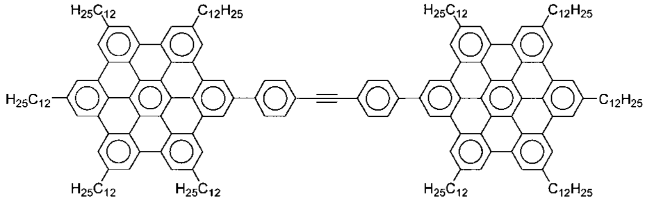

95

uents, a consequence of the much greater $\pi-\pi$-interaction of the repeat units. Swellable/partially soluble materials may be obtained by including further solubilizing groups in the main chain separating the superbenzene units as in the case of the polysiloxane **97**.[274] Likewise, monofunctionalized superbenzenes can be subjected to chain polymerization, leading to high molecular weight polymers carrying HBC units as pendant side groups. In the process of such "poly-HBC" synthesis it can be advantageous to utilize a kind of precursor route in which the polymerization is performed not for the functionalized HBC, but for the corresponding hexaphenylbenzene precursor, obviating solubility problems during the synthesis. Typical examples are the radical polymerization of vinyl and styryl derivatives of hexaphenylbenzenes yielding homopolymers and copolymers, **98** and **99**, with styrene and which can then be subjected to polymer-analogous cyclodehydrogenation reactions of the hexaphenylbenzene moieties.[274,275]

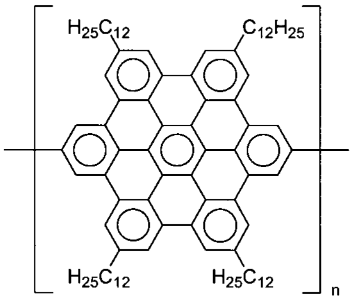

96

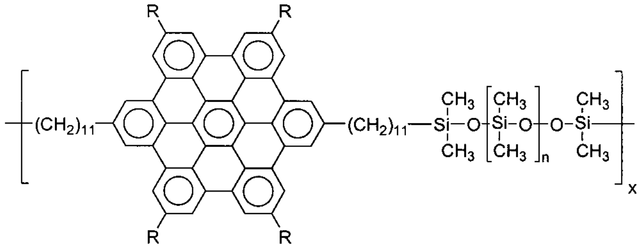

97

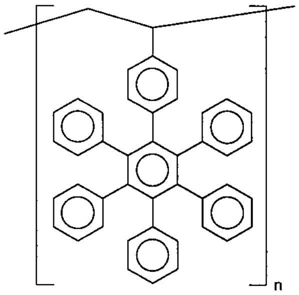

98

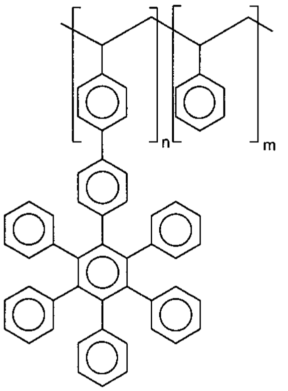

99

Why should one design a benzene-related chemistry by using a building block having 20 times the size of benzene? One answer is certainly related to the detection of single molecules (see section V) for which the size of the objects is crucial. Also, considering the extremely dilute concentrations employed in the particular case of single-molecule fluorescence spectroscopy, chromophores absorbing at much longer wavelengths (>400 nm) are required to allow detection in the presence of unavoidable, adventitious contaminants which absorb below this range.[47] This requirement is met by fusing superbenzenes to larger PBAHs creating larger π-systems. The other answer comes from the supramolecular aspects which have been discussed in section III.C. HBC disks tend to form aggregates with a face-to-face arrangement of the disks, both in solution and in the melt. Thus, the rigid-rod type poly-HBC **96** cannot only establish a $\pi-\pi$-interaction along the chain, but also, subject to the processing conditions, a $\pi-\pi$-interaction between the chains and thus increase the dimensionality of conjugation.[274] In a related fashion, the polysiloxane main-chain polymer **97** forms gels in all organic solutions because of some cross-linking due to interactions between the disks even though the monomeric superbenzene and the polysiloxane themselves are highly soluble.[274]

IV. Dendrimers from Benzene Repeat Units

There are many polymer architectures beyond chains such as stars, combs, and brushes. An example of a star-type oligophenylene is structure **100**.[276] It can be described as possessing three oligophenylene chains which have one central benzene ring in common. However, since the inner benzene ring and the six neighboring phenyl groups adopt a strongly twisted propeller-type arrangement, from the point of view of π-conjugation, molecule **100** can better be described as possessing six oligophenylene units of about one-half the size of the longest chain. A special topology is established in hyperbranched

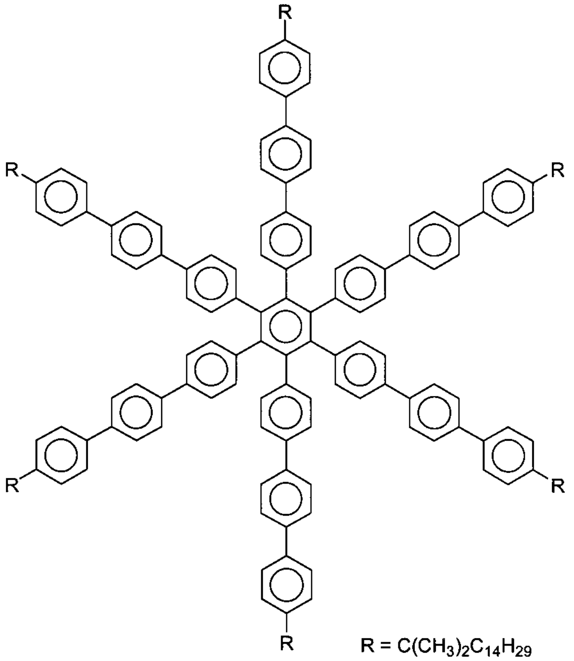

100

polymers **101**[45,53] which possess a high degree of branching but are not cross-linked. Such macromolecules become available when a AB$_n$-type molecule is subjected to polymerization reactions. AB$_n$ represents different chemical functions, A and B, in the monomer which occur in the ratio 1:n. If a reaction now occurs between two B functions of one monomer and the A functions of two other monomers, one expects a new molecule possessing only one A function but four B functions. When the sequence is performed repetitively, a macromolecule is formed which comprises a multitude of branches and B groups but only a single A group.

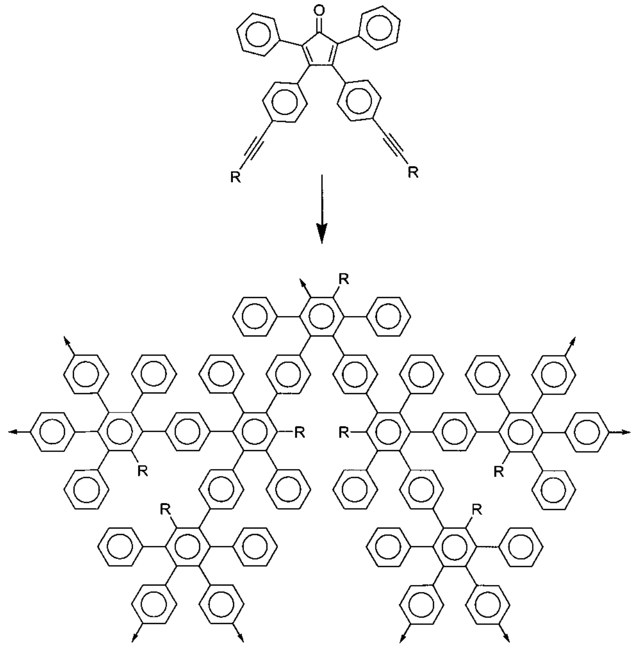

101

A discussion of the steric and statistical effects, which lead to the polydispersity and the occurrence of structural defects in the resulting hyperbranched polymer, is beyond the scope of this text. Let us, instead, consider a subgroup of hyperbranched polymers, the so-called dendrimers which exist as monodisperse and structurally perfect macromolecules with a regular branching pattern.[50−56,58,59,277] The synthesis of dendrimers is, of course, more demanding than that of hyperbranched polymers. A *divergent* approach is possible which starts from an inner core and proceeds via a generation-by-generation build up. In contrast, the *convergent* approach starts at the periphery of the dendrimer and rests upon the attachment of preformed branches to the core. The design and synthesis of dendrimers and their use as functional nanoparticles has created a tremendous challenge for chemistry whereby the spatial isolation of cores, inside the macromolecule, and the exponential multiplication of chemical functions at the surface are key aspects. Various growth reactions and branching structures have been employed.[8,45,278] Problems which have frequently appeared concern the chemical instability of some dendrimers and their conformational mobility. As a result of conformational changes among flexible arms, dendrimers,

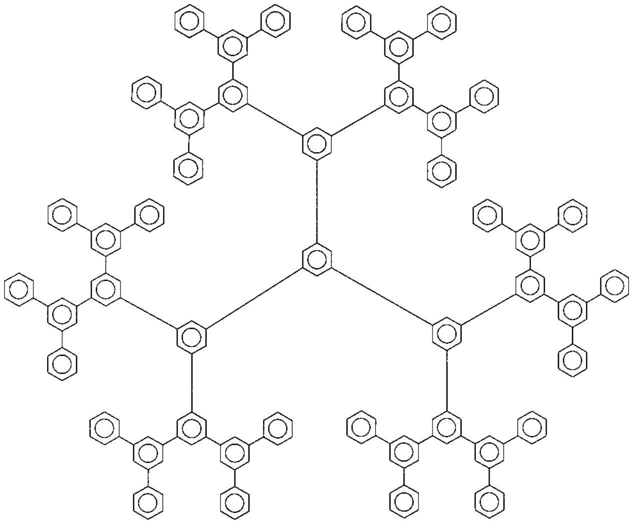

102

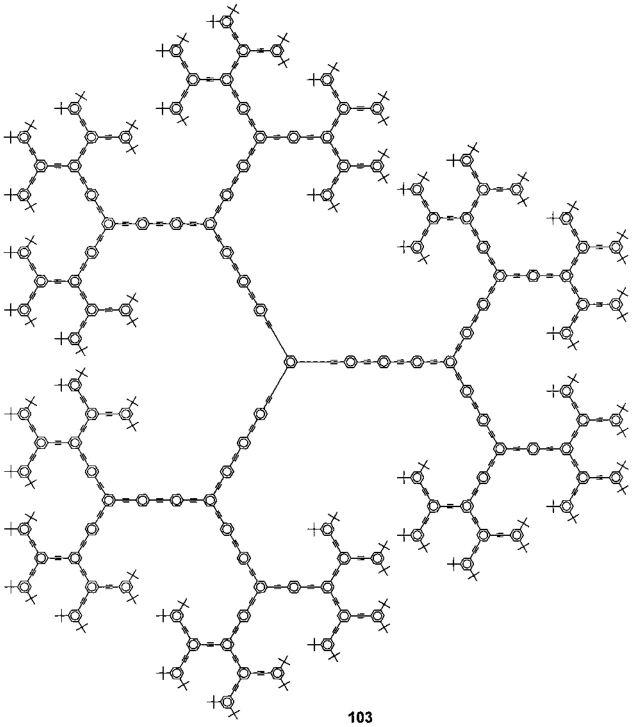

103

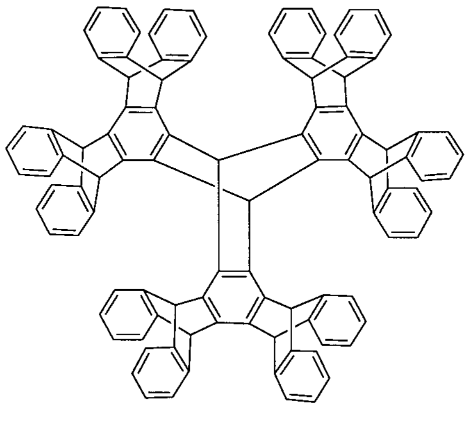

104

which are often depicted by a spherical structure, can adopt a totally different, e.g., flat shape which limits, of course, the spatial definition of peripheral chemical functions. These drawbacks have led to the construction of benzene-based dendrimers. Typical cases comprise 1,3,5-trisubstituted benzene repeat units **102**[63] or their analogues with additional ethynylene bonds **103**[64] as well as so-called iptycenes **104**.[279] A third dendrimer structure type[51−56,58,59,277] has been introduced comprised of pentaphenylbenzene repeat units leading to a tight packing of twisted, interlocked benzene rings. This interlocking has important consequences because the resulting dendrimers can be described by various pieces of evidence, e.g., NMR spectroscopy and atomic force microscopy, as shape-persistent macromolecules. Further, the choice of the core such as tetraphenylmethane, 3,3′,5,5′-biphenyl, or hexaphenylbenzene allows one to systematically change the shape of the resulting three-dimensional objects.[59,277]

The synthetic method applied is that of a repetitive Diels−Alder reaction whereby ethynyl-substituted tetraphenylcyclopentadienones **105** and **106** serve as branching reagents, since they contain one diene and two to four dienophile functions, respectively. The protection−deprotection sequence applied in the stepwise construction of generations will not be discussed here; the structural perfection of the resulting 3D polyphenylenes is, however, remarkable. Thus, a polyphenylene **107** containing, e.g., 302 benzene rings can be shown by MALDI-TOF mass spectrometry to be free of any structural defect.[278]

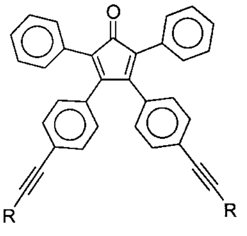

105

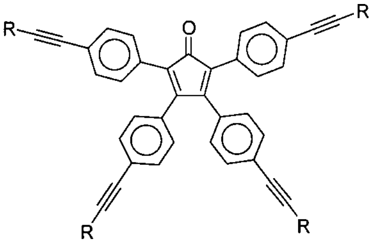

106

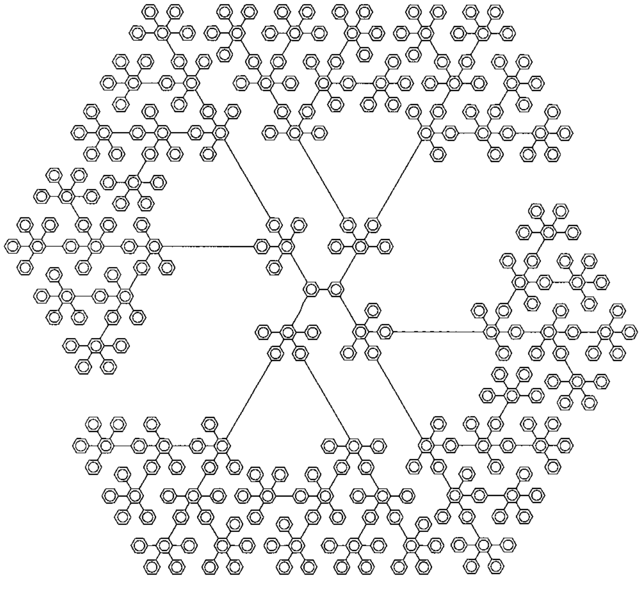

107

It is important to note that the polyphenylene macromolecules are colorless and soluble in organic solvents. Remarkably enough, the solubility even increases when going to higher generations. These properties can be explained by the occurrence of twisted benzene rings which excludes any extended π-conjugation and by the absence of π−π-stacking phenomena which obviously prevails in the 1D and 2D polyphenylenes ascribed above.

In the present macromolecular 3D polyphenylenes, the benzene ring adopts a new role: instead of laying the structural basis for extended π-conjugation, it only serves as a stable, regularly shaped branching point and space filler. The consequences of this function for the design of shape-persistent 3D macromolecules is immense and will be referred to in section V. If one wants to construct polyphenylene nanoparticles which can act as nanosized chromophores or electrophores, one has to incorporate additional π-conjugated groups. To obtain nanoemitters, structures such as **108** were synthesized where a light-emitting perylenetetracarboxylic acid diimide is surrounded by stable dendrons with variable sizes, producing emitters of different size.[280] These chromophoric molecules possess cores and shells with both high chemical and photochemical stability. The rigid shell is supposed to preclude any aggregation of the chromophore; this is important since aggregation often leads to fluorescence quenching and is responsible for photochemical destruction processes. Further, the dendronized dyes can now be blended into various host polymers, giving a high migrational fastness. Another nanoemitter design is possible if several chromophores, such as the perylenemonoimide **109**, are attached to the surface of the polyphenylene dendrimers giving rise to, e.g., **110**.[48,57,281,282]

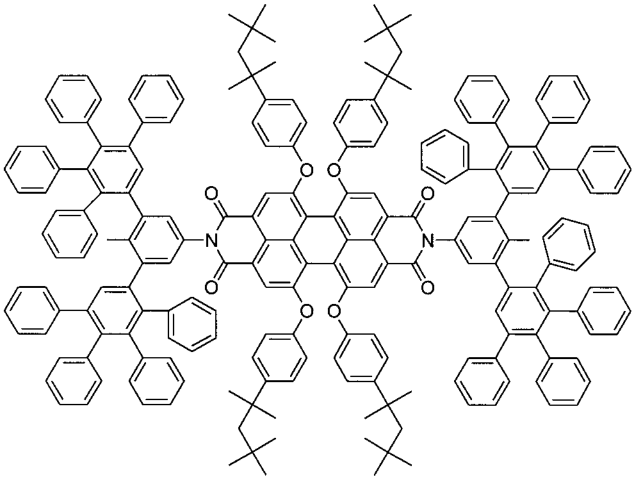

108

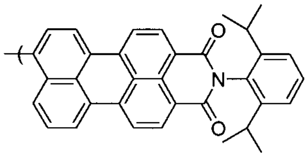

109

It is challenging to investigate whether the single fluorophores behave independently and whether an exchange of their excitation is possible. Even more

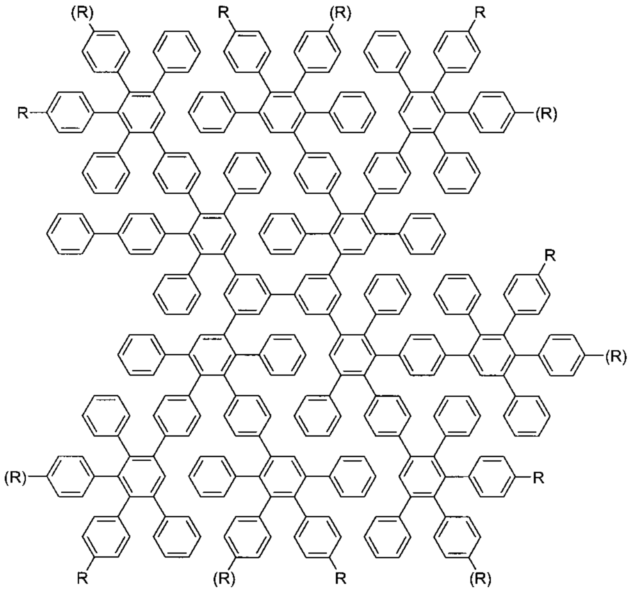

110

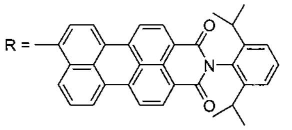

(R) = alternative position of substituent

demanding is the synthesis of dendrimer **111**,[280] which contains two different chromophores and is particularly made for allowing energy transfer inside the nanoparticle.[280] The visualization of *single* dendrimer nanoparticles by scanning probe techniques and their photophysical characterization by single-molecule spectroscopy are presented in section V.

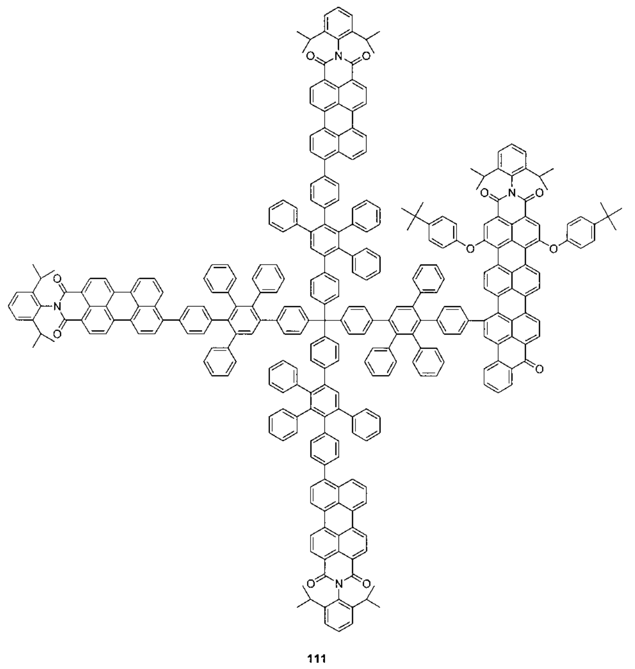

111

V. Single-Molecule Visualization of Nanosized Polyphenylenes and PBAHs

Lamellar patterns formed via the side-by-side arrangement of linear polyphenylenes[68] and columns built from face-to-face PAHs[157,161,237,242] have been described as typical supramolecular patterns of benzene-based macromolecules. Such ordered arrays of molecules are important for understanding many electrical and electrooptical properties. Further, they document the need for a more general view upon electronic structures which includes both intra- and intermolecular $\pi-\pi$-interaction. When dealing with supramolecular architectures, an immediate question concerns the persistence length of the prevailing motif and the spatial extension of the particular patterns. Such a view establishes a structural hierarchy which includes the initial formation of aggregates of a few molecules and proceeds to increasingly complex structures. The logical starting point of such considerations is the visualization of single molecules in real space. Scanning probe techniques, e.g., scanning tunneling microscopy[155,158,222,224,225,227,228,230,231,283,284] and atomic force microscopy,[285] are now available which allow such visualization in real space, and single-molecule spectroscopy[39,67] permits the detection of single fluorophores by their light emission. In many instances such experiments require the immobilization of the single molecules in a matrix or at a surface for which the above principles of self-organization are important.

The other design aspect concerns the question of how one can systematically modify the size and dimensionality of the molecular and macromolecular objects, and the reader will readily anticipate from what has been said above that the construction of oligo- and polyphenylenes is highly appropriate for that purpose. With benzene having a diameter of 0.28 nm and an inter-ring single bond being 0.15 nm long, a terphenyl chain is 1.14 nm long, which is also the diameter of hexaphenylbenzene **53**. Likewise, the above-mentioned polyphenylene dendrimer **107** which contains 302 benzene rings possesses a diameter of about 6.0 nm.[277,278] A single polyphenylene dendrimer such as **112** can be visualized by electron microscopy after shadowing with tungsten/tantalum alloy, yielding a perfectly circular projection and a medium diameter of 6.1 nm.[277] Dendrimer **112** has also been detected as a single object by AFM after deposition on a mica substrate surface from a very dilute solution. The diameter obtained from the height of single molecules (6.0 nm) corresponds very well to the values obtained by electron microscopy.[60] Interestingly, when a somewhat more concentrated solution of the dendrimer is used for film formation, one obtains single particles which possess a diameter of about 20 nm; thus, this seems to suggest a well-defined aggregation process. This experimentally obtained diameter corresponds to the values obtained from molecular simulation of this dendrimer under the assumption that the polyphenylene chains do not deform and the branches radiate away form the central point of the dendrimer.[277] The good agreement between the measured and the calculated diameter proves that no backfolding takes place in these molecules as is the case in dendrimers built up from aliphatic chains. The high density of benzene rings

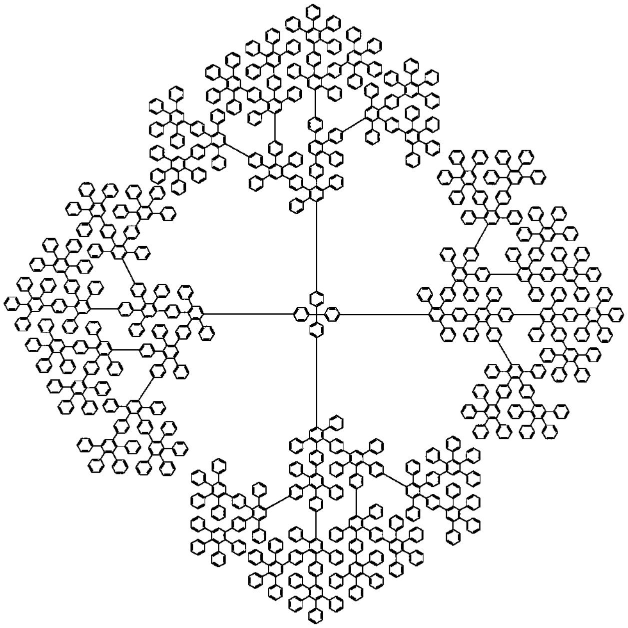

112

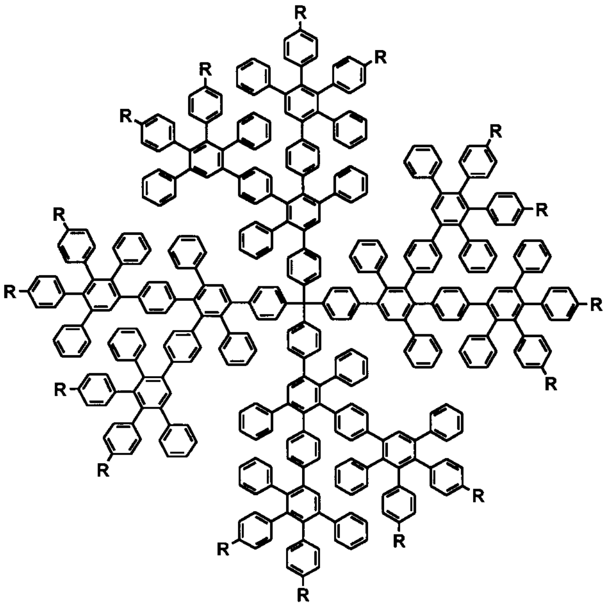

113

R= $C_{12}H_{25}$

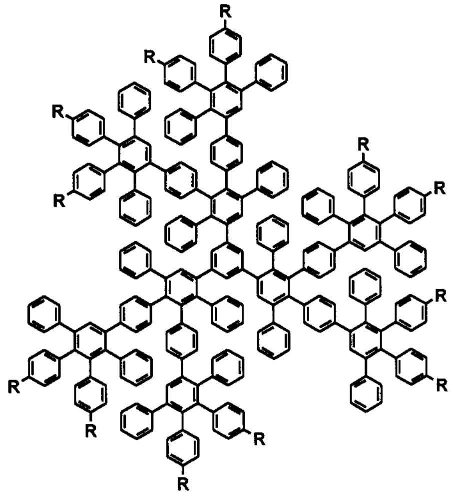

114

induce, furthermore, steric hindrance inside the dendrimer. This leads not only to an increased stiffness of the whole polyphenylene dendrimer scaffold, proven by solid-state dynamic NMR-measurements,[61] but also to a distinct shape persistence as seen by transmission electron microscopy and AFM.

Even more surprising is the formation of several hundred nm long organized structures of dendrimers on HOPG, formed upon spin coating of dendrimers such as **113** and **114** carrying additional alkyl chains on their surface.[62] For example, spin coating of dilute solutions of **113** yields regions with parallel stripes of 5.9 nm spacing. These regions are usually 50−100 nm wide and up to 800 nm long. On the other hand, spin coating of **114** yields two-dimensional hexagonally ordered crystals. The height of these molecules in both self-organized regions is slightly less than 1 nm smaller than the expected size of the dendritic molecules. This can be explained only with a kind of planarization of the dendrimers due to the strong attractive forces between the alkyl chains and the graphite surface. This leads to a bending of the main polyphenylene branches of the dendrimer. The stripe and the hexagonal packing can be explained analogously to three-dimensional organization as the formation of layered and hexagonal structures, respectively, due to the segregation of aliphatic and aromatic regions.

The dye-loaded dendrimer **110** can be detected by means of single-molecule fluorescence.[48,57,281,282] This multichromophoric system was embedded into a thin polymeric film at very low concentrations so that individual dendrimer molecules could be studied by far-field fluorescence microscopy at room temperature. Temporal fluorescence intensity fluctuations, fluorescence spectra, and decay times were measured separately or simultaneously. Collective on/off jumps of the fluorescence intensity as well as different emissive levels were observed for single dendrimer molecules with eight perylenemonoimide chromophores at the outer rim. Owing to the outstanding photostability of the perylene dyes, the fluorescence intensity trajectory exhibits a mean survival time of 450 s, containing an average of 1.1×10^6 detected photons. Measuring spectra and decay times reveals the presence of both noninteracting and dimer-like interacting chromophoric sites within an individual dendrimer. It was also possible to observe the transition between these two different spectral forms and decays on one molecule. These results underline the dynamic character of interactions among the chromophores. Furthermore, the single-molecule data prove the assumptions elaborated for bulk measurements.

The tetraphenoxyperylenediimide chromophore **115**[280] is very well suited for SMS measurements due to its extraordinary stability. Single molecules could be studied on an average for more than 1000 s.

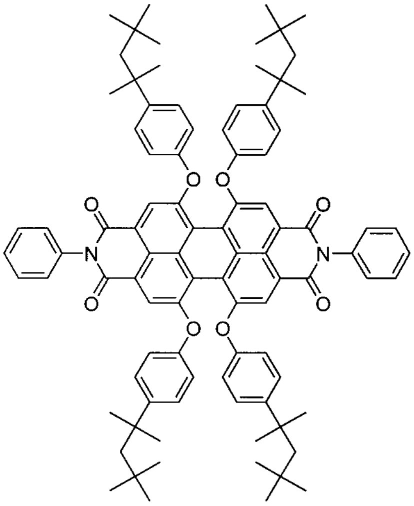

115

Recording numerous fluorescence spectra shows a bimodal distribution of the peak position due to conformational changes within the chromophore. Attaching polyphenylene dendrons to this perylenediimide system influences this distribution and the position of the peaks. Here, SMS was used to monitor conformational interconversions on the single-molecule level.

As mentioned earlier, PBAHs such as **22**[155] and **88**[46] could be deposited onto substrate surfaces such as highly ordered pyrolytic graphite or molybdenum sulfide under formation of ordered monolayers with characteristic lattice parameters. For HBC **22**, images with up two 12 bright spots (per molecule) showing 3-fold symmetry orientation were obtained. The contrast of these images is independent of the tunnel voltage in a broad range of $+$ 1.0 to $-$ 1.0 V. The attempt to explain this phenomenon by taking the HOMO and/or LUMO levels of a free HBC molecule into account were not totally conclusive.[230] In the case of the "superbiphenyl" **94**, both "superbenzene" subunits of each molecule are clearly visualized as a ring-like pattern surrounding a single bright spot (the central benzene ring of each subunit).[225] Further, the measured distance between these two central benzene rings corresponded exactly with the expected value. While STM measurements could not conclusively detect the degree of torsion between the connected disks, energy minimization calculations were utilized to estimate the situation on the graphite surface.

While the physical origin of contrast formation is not yet fully understood, it is important that in the higher homologues of HBC **22**, i.e., **70**[224] and **71**,[284] the STM pictures reveal bright stripes for the longest oligophenyl chains together with a lower current for the areas for which frontier orbitals possess nodal planes. This is exciting because it would imply a direct visualization of a molecular orbital. What is even more important from a point of view of an elementary MO theory is the fact that one can record current−potential curves separately for aliphatic and aromatic domains.[155] Therefore, the "aliphatic curve" is more or less symmetric, i.e., the tunnel current is not enhanced by a coupling to the frontier orbitals. This is, of course, not surprising in view of the large energy difference between the latter and the Fermi energy of the electrodes. This is no longer true when the U-curve is recorded over the aromatic core, since it now adopts a strongly asymmetric, diode-like shape. Preliminary experiments of the higher homologues **70** and **71** allow a systematic comparison of the current−potential curves for structurally related molecules.[160,284] They reveal a systematic change of the shape of the curves which can be correlated with conventional (bulk) information obtained for the energies of frontier orbitals by electron absorption spectroscopy and cyclic voltammetry.

The direct visualization in real space of PAHs of suitable size by scanning tunneling microscopy thus opens a new way for the description of the bonding situation. An important step beyond the visualization is, of course, the detection of single-molecule functions, such as light emission and energy transfer or current rectification. The challenge for future research is, of course, to proceed to more complex electronic functions of single molecules, such as current amplification or writing information on single molecules, as an approach toward information storage. In any event, before one talks about technology, one needs to know the science and the characterization of benzene-based 1D, 2D, and 3D molecular objects by scanning tunneling microscopy, and single-molecule spectroscopy is an exciting way of understanding and utilizing single-molecule function.

VI. Conclusion

Classical aromaticity discussions have in the past brought together theoreticians, spectroscopists, and synthetic chemists. It has been our concern to further widen the view at aromaticity. In any attempts at understanding cyclic π-conjugation in organic molecules, further interdisciplinary interaction is promoted by covering larger and larger π-systems and eventually conjugated polymers. The chemistry and physics of conjugated polymers has developed into a science and technology of electronic materials. However, even if the reader tends to confine his view to the fundamental aspects of π-conjugated structures, it is clear that extended π-systems create challenging problems for any discussions into π-structure. The other important aspect is that while being concerned with π-conjugation, one should not restrict the attention to intramolecular aspects. Properties such as the color of absorbed and emitted light or charge-carrier transport which are regarded as being characteristic for conjugated systems cannot be understood when concentrating one's focus on the behavior of small isolated molecules in dilute solution.

VII. References

(1) Krygowski, T. M.; Cyranski, M. K.; Czarnocki, Z.; Häfelinger, G.; Katritzky, A. R. *Tetrahedron* **2000**, *56*, 1783−1796.
(2) Trujillo, J. M.; Jorge, R. E.; Navarro, E.; Boada, J. *Phytochemistry* **1990**, *29*, 2991−2993.
(3) Seong, B. L.; Han, M. L. *Chem. Lett.* **1982**, 627−628.
(4) Martin, R. E.; Diederich, F. *Angew. Chem., Int. Ed. Engl.* **1999**, *38*, 1350−1377; *Angew. Chem.* **1999**, *111*, 1440−1469.

(5) Sastri, V. R.; Schulman, R.; Robert, D. C. *Macromolecules* **1982**, *15*, 939.
(6) Hart, H.; Luo, J. *J. Org. Chem.* **1987**, *30*, 4833.
(7) Garratt, P. J. *Aromaticity*; John Wiley and Sons: New York, 1986.
(8) Inoue, K. *Prog. Polym. Sci.* **2000**, *25*, 453–571.
(9) Kobayashi, S. *Catalysis in Precision Polymerization*; John Wiley and Sons: West Sussex, 1997.
(10) Soos, Z. G.; Mukhopadhyay, D.; Painelli, A.; Girlando, A. *Handbook of Conducting Polymers*, 2nd ed.; Marcel Decker: New York, 1998.
(11) Schlüter, A. D. *Handbook of Conducting Polymers*, 2nd ed.; Marcel Decker: New York, 1998.
(12) Igbal, Z.; Ivory, D. M.; Marti, J.; Brédas, J. L.; Baughman, R. H. *Mol. Cryst. Liq. Cryst.* **1985**, *118*, 103.
(13) Kaplan, M. L.; Schmidt, P. H.; Chen, C. H.; Walsh, J. M. W. *Appl. Phys. Lett.* **1980**, *36*.
(14) Brédas, J. L.; Baughman, R. H. *J. Chem. Phys.* **1985**, *83*, 1316.
(15) Pommerantz, M.; Cardona, R.; Rooney, P. *Macromolecules* **1989**, *22*, 304.
(16) Lahti, P. M.; Obrzut, J.; Karasz, F. E. *Macromolecules* **1987**, *20*, 2023.
(17) Barber, J.; Siddigui, J. A. *Abstr. Pap. Am. Chem. Soc.* **1998**, *A215: U440*, Pt2.
(18) Hill, H. W. *High Performance Polymers: Their Origin and Development*; Elsevier: New York, 1986.
(19) Freund, L.; Heitz, W. *Makromol. Chem.* **1990**, *191*, 815.
(20) Mullins, M. J.; Woo, E. P. *J. Makromol. Sci., Rev. Macromol. Chem. Phys.* **1987**, *C27*, 313.
(21) Hoffmann, U.; Helmer-Metzmann, F.; Klapper, M.; Müllen, K. *Macromolecules* **1994**, *27*, 3575–3579.
(22) Neuse, E. W. *Adv. Polym. Sci.* **1982**, *47*, 1–42.
(23) Chung, T. S. *J. Macromol. Sci., Rev. Macromol. Chem.* **1997**, *C37*, 277–301.
(24) Inzelt, G.; Pineri, M.; Schultze, J. W.; Vorotyntsev, M. A. *Electrochim. Acta* **2000**, *45*, 2403–2421.
(25) Kerres, J.; Ullrich, A.; Haring, T.; Baldauf, M.; Gebhardt, U.; Preidel, W. *J. New Mater. Electrochem. Syst.* **2000**, *3*, 229–239.
(26) Braun, T.; Schubert, A. P.; Kostoff, R. N. *Chem. Rev.* **2000**, *100*, 23–37.
(27) Ajayan, P. M. *Chem. Rev.* **1999**, *99*, 1787–1799.
(28) de Heer, W. A. *Curr. Opin. Solid State. Mater. Sci.* **1999**, *4*, 355–359.
(29) Saito, Y. *New Diamond Front. Carbon Technol.* **1999**, *9*, 1–30.
(30) Peebles, L. H. *Int. Mater. Rev.* **1994**, *39*, 75–92.
(31) Umemoto, T.; Satani, S.; Sakata, Y.; Misumi, S. *Tetrahedron Lett.* **1975**, 3159.
(32) Iwama, A.; Toyoda, T.; Yoshida, M.; Otsubo, T.; Sakata, Y.; Misumi, S. *Bull. Chem. Soc. Jpn.* **1978**, *51*, 2988.
(33) *Handbook of Liquid Crystals*; Demus, D., Goodby, J. W., Gray, G. W., Spiess, H. W., Vill, V., Eds.; Wiley-VCH: Weinheim, 1998.
(34) Oberlin, A.; Bonnamy, S.; Rouxhet, P. G. *Chem. Phys. Carbon* **1988**, *26*, 1–148.
(35) Motta, O.; DiMario, L.; Incarnato, L.; Acierno, D. *Polymer* **1996**, *37*, 2373–2377.
(36) Chand, S. *J. Mater. Chem.* **2000**, *35*, 1303–1313.
(37) Kraft, A.; Grimsdale, A. C.; Holmes, A. B. *Angew. Chem., Int. Ed.* **1998**, *37*, 402–428; *Angew. Chem.* **1998**, *110*, 416–443.
(38) Ambrose, W. P.; Goodwin, P. M.; Jett, H.; Van Orden, A.; Werner, J. H.; Keller, R. A. *Chem. Rev.* **1999**, *99*, 2929–2956.
(39) Tamarat, P.; Maali, A.; Lounis, B.; Orrit, M. *J. Phys. Chem. A* **2000**, *104*, 1–16.
(40) Harada, Y.; Funatsu, T.; et al. *Methodol. Cell Biol.* **1998**, *55*.
(41) Luo, X. O.; Yu, M.; Huang, H.; Ruoff, R. S. *Nanotechnology* **1999**, *10*, 269–272.
(42) Schlüter, A. D.; Rabe, J. P. *Angew. Chem., Int. Ed.* **2000**, *39*, 864–883; *Angew. Chem.* **2000**, *112*, 860–880.
(43) Scherf, U. *Top. Curr. Chem.* **1999**, *201*, 163–222.
(44) Bunz, U. H. F. *Chem. Rev.* **2000**, *100*, 1605–1644.
(45) Berresheim, A. J.; Müller, M.; Müllen, K. *Chem. Rev.* **1999**, *99*, 1747–1785.
(46) Müller, M.; Kübel, C.; Müllen, K. *Chem. Eur. J.* **1998**, *4*, 2099–2109.
(47) Gensch, T.; Hofkens, J.; Heirmann, A.; Tsuda, K.; Verheijen, W.; Vosch, T.; Christ, T.; Basché, T.; Müllen, K.; De Schryver, F. C. *Angew. Chem., Int. Ed. Engl.* **1999**, *38*, 3752–3756; *Angew. Chem.* **1999**, *111*, 3970–3974.
(48) Hofkens, J.; Maus, M.; Gensch, T.; Vosch, T.; Cotlet, M.; Köhn, F.; Herrmann, A.; Müllen, K.; De Schryver, F. *J. Am. Chem. Soc.* **2000**, *122*, 9278–9288.
(49) Shifrina, Z. B.; Averina, M. S.; Rusanov, A. L.; Wagner, M.; Müllen, K. *Macromolecules* **2000**, *33*, 3525–3529.
(50) Fischer, M.; Vögtle, F. *Angew. Chem., Int. Ed. Engl.* **1999**, *38*, 885–905; *Angew. Chem.* **1999**, *111*, 934–955.
(51) Morgenroth, F.; Reuther, E.; Müllen, K. *Angew. Chem., Int. Ed. Engl.* **1997**, *36*, 631–634; *Angew. Chem.* **1997**, *109*, 647–649.
(52) Kübel, C.; Morgenroth, F.; Müllen, K. *J. Mater. Chem.* **1997**, *7*, 1207–1211.
(53) Morgenroth, F.; Müllen, K. *Tetrahedron* **1997**, *53*, 15349–15366.
(54) Morgenroth, F.; Wagner, M.; Berresheim, A.; Müllen, K. *Chem. Commun.* **1998**, 1139–1140.
(55) Morgenroth, F.; Kübel, C.; Müller, M.; Wiesler, U. M.; Berresheim, A. J. *Carbon* **1998**, *36*, 833–837.
(56) *Conjugated polymers, oligomers and dendrimers: From polyacetylene to DNA*; Leuninger, J., Müllen, K., Eds.; De Boeck: Louvain-la-Neuve, 1999; Vol. 4.
(57) Hofkens, J.; Latterini, L.; De Belder, G.; Gensch, T.; Maus, M.; Vosch, T.; Karni, Y.; Schweitzer, G.; De Schryver, F. C.; Herrmann, A.; Müllen, K. *Chem. Phys. Lett.* **1999**, *304*, 1–9.
(58) Brocorens, P.; Zojer, E.; Cornil, J.; Shuai, Z.; Leising, G.; Müllen, K.; Brédas, J. L. *Synth. Met.* **1999**, *100*, 141–162.
(59) Wiesler, U.-M.; Müllen, K. *Chem. Commun.* **1999**, 2293–2294.
(60) Zhang, H.; Grim, P. C. M.; Foubert, P.; Vosch, T.; Vanoppen, P.; Wiesler, U.-M.; Berresheim, A. J.; Müllen, K.; Schryver, F. C. D. *Langmuir* **2000**, *16*, 9009–9014.
(61) Wind, M.; Wiesler, U. M.; Saalwächter, K.; Müllen, K.; Spiess, H. W. Manuscript in preparation.
(62) Loi, S.; Wiesler, U. M.; Butt, H. J.; Müllen, K. *Chem. Commun.* **2000**, 1169.
(63) Miller, T. M.; Neenan, T. X.; Zayas, R.; Bair, H. E. *J. Am. Chem. Soc.* **1992**, *114*, 1018.
(64) Xu, Z.; Moore, J. S. *Acta Polym.* **1994**, *45*, 83.
(65) Vacha, M.; Tani, T. *J. Phys. Chem. A* **1997**, *101*, 5027–5030.
(66) Göhde, W.; Fischer, U. C.; Fuchs, H.; Tittel, J.; Basché, T.; Bräuchle, C.; Herrmann, A.; Müllen, K. *J. Phys. Chem.* **1998**, *102*, 9109–9116.
(67) Plakhotnik, T.; Donley, E. A.; Wild, U. P. *Annu. Phys. Chem.* **1997**, *48*, 181–212.
(68) Müllen, K.; Wegner, G. *Electronic Materials: The Oligomer Approach*; Wiley-VCH: Weinheim, 1998.
(69) Cacialli, F. *Curr. Opin. Colloid Interface Sci.* **1999**, *4*, 159–164.
(70) Blom, P. W. M.; Vissenberg, M. C. J. M. *Mater. Sci. Eng. R.* **2000**, *27*, 53–94.
(71) McQuade, D. T.; Pullen, A. E.; Swager, T. M. *Chem. Rev.* **2000**, *100*, 2537–2574.
(72) Cailleaau, H.; Baudour, J. L.; Meinnel, J.; et al. *Faraday Discuss. Chem. Soc.* **1980**, *69*, 7.
(73) Tsuzuki, S.; Tanabe, K. *J. Phys. Chem.* **1991**, *95*, 139.
(74) van Hutten, P. F.; Hadziioannou, G. *Handbook of Organic Conductive Molecules and Polymers*; John Wiley and Sons: Chichester, 1997.
(75) Socci, E. P.; Farmer, B. L.; Baker, K. N.; et al. *Polymer* **1993**, *34*, 1571–1587.
(76) Vanhee, S.; Rulken, R.; Lehmann, U.; Rosenauer, C.; Schulze, M.; Köhler, W.; Wegner, G. *Macromolecules* **1996**, *29*, 5136–5142.
(77) Petekidis, G.; Vlassopoulus, D.; Galda, P.; Reham, M.; Ballauff, M. *Macromolecules* **1996**, *29*, 9.
(78) Hickl, P.; Balhauff, M.; Scherf, U.; Müllen, K.; Lindner, P. *Macromolecules* **1997**, *30*, 273–279.
(79) Cotts, P. M.; Swager, T. M.; Zhou, Q. *Macromolecules* **1996**, *29*, 7323–7328.
(80) Grell, M.; Bradley, D. D. C.; Long, X.; Chamberlain, T.; Inbasekaran, M.; Woo, E. P.; Soliman, M. *Acta Polym.* **1998**, *49*, 439–444.
(81) Hiemez, P. C. *Polymer Chemistry The Basic Concepts*; Marcel Decker: New York, 1984.
(82) Mattice, W. L.; Suter, U. W. *Conformational Theory of Large Molecules*; John Wiley ans Sons: New York, 1994.
(83) Elias, H. G. *An Introduction to Polymer Science*; VCH: Weinheim, 1997.
(84) Farmer, B. L.; Chapman, B. R.; Dudis, D. S.; Adams, W. W. *Polymer* **1993**, *34*, 1588–1601.
(85) Vaia, R. A.; Dudis, D.; Henes, J. *Polymer* **1998**, *39*, 6021–6036.
(86) Grim, P. C. M.; DeFreyter, S.; Gesquiére, A.; et al. *Angew. Chem., Int. Ed.* **1997**, *36*, 2601–2603; *Angew. Chem.* **1997**, *109*, 2713–2715.
(87) Ambrosch-Draxl, C.; Majewski, J. A.; Vogl, P.; Leising, G. *Phys. Rev. B* **1995**, *51*, 9668.
(88) Pena, D.; Cobas, A.; Pérez, D.; Guitián, E.; Castedo, L. *Org. Lett.* **2000**, *2*, 1629–1632.
(89) Miao, M. S.; Van Camp, P. E.; Van Doren, V. E.; Ladik, J. J.; Mintmire, J. W. *J. Chem. Phys.* **1998**, *109*, 9263–9231.
(90) Bredas, J. L.; Street, G. B.; Themans, B.; Andre, J. M. *J. Chem. Phys.* **1985**, *83*, 1323–1329.
(91) Gregorius, H.; Heitz, W.; Müllen, K. *Adv. Mater.* **1993**, *5*, 279–281.
(92) Scherf, U. *Handbook of Conducting Polymers*, 2nd ed.; Marcel Decker: New York, 1998.
(93) Scherf, U.; Müllen, K. *Makromol. Chem. Rapid Commun.* **1991**, *12*, 489.
(94) Scherf, U.; Müllen, M. *Adv. Polym. Sci.* **1995**, *123*, 1–40.
(95) Klarner, G.; Lee, J. I.; Lee, V. Y.; et al. *Chem. Mater.* **1999**, *11*, 1800–1805.
(96) Marsitzky, D.; Klapper, M.; Müllen, K. *Macromolecules* **1999**, *32*, 8686–8688.
(97) Gross, M.; Muller, D. C.; Nothofer, H. G. *Nature* **2000**, *405*, 661–665.

(98) Millard, I. S. *Synth. Met.* **2000**, *111*, 119−123.
(99) Donat-Bouillud, A.; Levesque, I.; Tao, Y.; et al. *Chem. Mater.* **2000**, *12*, 1931−1936.
(100) Blondin, P.; Bouchard, J.; Beaupre, S. *Macromolecules* **2000**, *33*, 5874−5879.
(101) Setayesh, S.; Marsitzky, D.; Müllen, K. *Macromolecules* **2000**, *33*, 1734−1736.
(102) Silva, C.; Russell, D. M.; Stevens, M. A.; et al. *Chem. Phys. Lett.* **2000**, *319*.
(103) Rumi, M.; Zerbi, G.; Scherf, U.; et al. *Chem. Phys. Lett.* **1997**, *273*, 429−434.
(104) Kreyenschmidt, M.; Uckert, F.; Müllen, K. *Macromolecules* **1995**, *28*, 4577.
(105) Leising, G.; Tasch, S.; Graupner, W. *Handbook of Conducting Polymers*, 2nd ed.; Marcel Decker: New York, 1998.
(106) Meier, H.; Stalmach, U.; Kolshorn, H. *Acta Polym.* **1997**, *48*, 379−384.
(107) Sun, J. Z.; Wu, F.; Tian, W. J.; Ma, Y. G.; Chen, Y.; Shen, J. C. *Chin. J. Chem.* **2000**, *18*, 465−499.
(108) Xu, B. B.; Zhang, J. H.; Peng, Z. H. *Synth. Met.* **2000**, *113*, 35−38.
(109) Setayesh, S.; Marsitzky, D.; Müllen, K. *Macromolecules* **2000**, *33*, 2016−2020.
(110) Wong, M. S.; Li, Z. H.; Shek, M. F.; Chow, K. H.; Tao, Y.; D'Iiorio *J. Mater. Chem.* **2000**, *10*, 1805−1810.
(111) Remmers, M.; Muller, B.; Martin, K.; Rader, H. J.; Kohler, W. *Macromolecules* **1999**, *32*, 1073−1079.
(112) Grimme, J.; Kreyenschmidt, M.; Uckert, F.; Müllen, K.; Scherf, U. *Adv. Mater.* **1995**, *7*, 292−295.
(113) Friend, R. H.; Gymer, R. W.; Holmes, A. B.; et al. *Nature* **1999**, *397*, 121−128.
(114) Mitschke, U.; Bäuerle, P. *J. Mater. Chem.* **2000**, *10*, 1507.
(115) Salaneck, W. R.; Friend, R. H.; Brédas, J. L. *Phys. Rev.* **1999**, *319*, 232−251.
(116) Bogdal, D.; Boron, A. *Polimery* **1999**, *44*, 646−655.
(117) Reddinger, J. L.; Reynolds, J. R. *Adv. Polym. Sci.* **1999**, *145*, 57−122.
(118) Greiner, A. *Polym. Adv. Technol.* **1998**, *9*, 371−389.
(119) Segura, J. L. *Acta Polym.* **1998**, *49*, 319−344.
(120) Remmers, M.; Schulze, M.; Wegner, G. *Macromol. Rapid. Commun.* **1996**, *17*, 239.
(121) Remmers, M.; Neher, D.; Grüner, J.; et al. *Macromolecules* **1996**, *23*, 7432.
(122) Conwell, E. *Trends Polym. Sci.* **1997**, *5*, 218−222.
(123) Kalinowski, D. *J. Phys. D, Appl. Phys.* **1999**, *32*, R179−R249.
(124) Vahlenkamp, T.; Wegner, G. *Macromol. Chem. Phys.* **1994**, *195*, 1933.
(125) Lauter, U.; Meyer, W. H.; Wegner, G. *Macromolecules* **1997**, *30*, 2092.
(126) Lauter, U.; Meyer, W. H.; Enkelmann, V.; Wegner, G. *Macromol. Chem. Phys.* **1998**, *199*, 2129.
(127) Steiner, O. B.; Rehan, M.; Caseri, W. R.; Suter, U. W. *Macromolecules* **1994**, *27*, 1983.
(128) Marsitzky, D.; Müllen, K. *20 Years of Synthetic metals−The role of synthesis*; Elsevier: Amsterdam, 1999.
(129) Pomerantz, M. *Handbook of Conducting Polymers*, 2nd ed.; Marcel Decker: New York, 1998.
(130) Bredas, J. L. *J. Chem. Phys.* **1985**, *82*, 3808.
(131) Schoenberg, M. *J. Chem. Soc.* **1935**, 1403−1404.
(132) Scherf, U. *Synth. Met.* **1993**, *55*−*57*, 767−772.
(133) Scherf, U.; Müllen, K. *Polymer* **1992**, *33*, 24432446.
(134) Beck, A.; Gompper, R.; Polborn, K.; Wagner, H. U. *Angew. Chem., Int. Ed. Engl.* **1993**, *32*, 1424−1426; *Angew. Chem.* **1993**, *105*, 1424−1426.
(135) Reisch, H.; Wiesler, U.; Scherf, U.; Tuytuylkov, N. *Macromolecules* **1996**, *29*, 8204−8210.
(136) Biermann, D.; Schmidt, W. *J. Am. Chem. Soc.* **1990**, *102*, 2.
(137) Graham, R. J.; Paquette, L. A. *J. Org. Chem.* **1995**, *60*, 5770.
(138) Brown, A. R.; Pomp, A.; deLeeuw, D. M.; et al. *J. Appl. Phys.* **1996**, *79*, 2136.
(139) Müllen, K. *Chem. Rev.* **1984**, *84*, 603−646.
(140) Friend, R. H. *Handbook of Conducting Polymers*, 2nd ed.; Marcel Decker: New York, 1998.
(141) Hopf, H. *Angew. Chem., Int. Ed. Engl.* **1984**, *23*, 948−960; *Angew. Chem.* **1984**, *96*, 947−959.
(142) Zander, M. *Polycyclische Aromaten*; Teubner: Stuttgart, 1995.
(143) Clar, E. *The Aromatic Sextet*; John Wiley and Sons: London, 1972.
(144) Franck, H. G.; Stadelhofer, J. W. *Industrielle Aromatenchemie*; Springer-Verlag: Heidelberg, 1987.
(145) Allen; Pingert *J. Am. Chem. Soc.* **1942**, *64*, 1365−1371.
(146) Hansch; Geiger *J. Org. Chem.* **1958**, *23*, 477.
(147) Harvey, R. G. *Polycyclic Aromatic Hydrocarbons*; Wiley-VCH: New York, 1997.
(148) Venediktov, E. A.; Perfilev, V. A.; Berezin, B. D. *Russ. J. Phys. Chem. (Engl. Trans.)* **1985**, *59*, 1824−1826.
(149) Cerutti; Martinet *C. R. Hebd. Seances. Acad. Sic.* **1953**, *237*, 1014.
(150) Berg, O.; Chronister, E. L. *J. Chem. Phys.* **1997**, *106*, 4401−4408.
(151) Koch, K. H.; Fahnenstich, U.; Baumgarten, M.; Müllen, K. *Synth. Met.* **1991**, *41*−*43*, 1619−1622.
(152) Schrader, S.; Koch, K. H.; Mathy, A.; Bubeck, K.; Müllen, K.; Wegner, G. *Synth. Met.* **1991**, *41*−*43*, 3223−3226.
(153) Stein, S. E.; Brown, R. L. *J. Am. Chem. Soc.* **1987**, *109*, 3721.
(154) Stein, S. E.; Brown, R. L. *Pathways to Graphite: Properties of Very large Polybenzoide Hydrocarbons*; VCH−Verlag: Weinheim, 1987.
(155) Stabel, A.; Herwig, P.; Müllen, K.; Rabe, J. P. *Angew. Chem., Int. Ed.* **1995**, *34*, 1609−1611; *Angew. Chem.* **1995**, *107*, 1768−1770.
(156) Brown, S. P.; Schnell, I.; Brand, J. D.; Müllen, K.; Spiess, H. W. *J. Am. Chem. Soc.* **1999**, *121*, 6712−6718.
(157) Fechtenkötter, A.; Saalwächter, K.; Harbison, M. A.; Müllen, K.; Spiess, H. W. *Angew. Chem., Int. Ed. Engl.* **1999**, *38*, 3039−3042; *Angew. Chem.* **1999**, *111*, 3224−3228.
(158) Ito, S.; Wehmeier, M.; Brand, J. D.; Kübel, C.; Epsch, R.; Rabe, J. P.; Müllen, K. *Chem. Eur. J.* **2000**, *6*, 4327.
(159) Halleux, A.; Martin, R. H.; King, G. S. D. *Helv. Chim. Acta* **1958**, *41*, 1177−1182.
(160) Iyer, V. S.; Wehmeier, M.; Brand, J. D.; Keegstra, M. A.; Müllen, K. *Angew. Chem., Int. Ed. Engl.* **1997**, *36*, 1604−1607; *Angew. Chem.* **1997**, *109*, 1675−1679.
(161) Herwig, P.; Kayser, C. W.; Müllen, K.; Spiess, H. W. *Adv. Mater.* **1996**, *8*, 510−513.
(162) Iyer, V. S.; Müllen, K. Manuscript in preparation.
(163) Dötz, F.; Müllen, K. Manuscript in preparation.
(164) Fechtenkötter, A.; Tchebotareva, N.; Watson, M.; Müllen, K. *Tetrahedron* **2001**, in press.
(165) Rumi, M.; Zerbi, G.; Müllen, K.; Müller, G.; Rehahn, M. *J. Chem. Phys.* **1997**, *106*, 24−34.
(166) Haigh, C. W.; Mallion, R. B. *Prog. Nucl. Magn. Reson. Spectrosc.* **1979**, *13*, 303−344.
(167) Mitchell, R. H.; Iyer, V. S. *J. Am. Chem. Soc.* **1996**, *118*, 2903−2906.
(168) Zhou, Z. X. *Int. Rev. Phys. Chem.* **1992**, *11*, 243−261.
(169) Shetty, A. S.; Zhang, J.; Moore, J. S. *J. Am. Chem. Soc.* **1996**, *118*, 1019−1027.
(170) Shetty, A. S.; Fischer, P. R.; Storck, K. F.; Bohn, P. W.; Moore, J. S. *J. Am. Chem. Soc.* **1996**, *118*, 9409−9414.
(171) Laali, K. K.; Tanaka, M.; Mitchell, R. H.; Lau, D. K. Y. *J. Org. Chem.* **1998**, *63*, 3059−3066.
(172) Brand, J. D. Ph.D. Thesis, University of Mainz, 2000.
(173) Ochsenfeld, C. *Phys. Chem. Chem. Phys.* **2000**, *2*, 2153-2159.
(174) Ochsenfeld, C.; Brown, S. P.; Schnell, I.; Gauss, J.; Spiess, H. W. *J. Am. Chem. Soc.*, submitted for publication.
(175) Burley, S. K.; Petsko, G. A. *Adv. Protein. Chem.* **1988**, *39*, 125.
(176) Hunter, C. A.; Singh, J.; Thornton, J. M. *J. Mol. Biol.* **1991**, *218*, 837.
(177) Brown, N. M. D.; Swinton, F. L. *J. Chem. Soc., Chem. Commun.* **1974**, 770.
(178) Hernández-Trujillo, J.; Costas, M.; Vela, A. *J. Chem. Soc., Faraday Trans.* **1993**, *89*, 2441.
(179) Brown, S. P.; Schnell, I.; Brand, J. D.; Müllen, K.; Spiess, H. W. *J. Mol. Struct.* **2000**, *521*, 179−195.
(180) Brown, S. P.; Schnell, I.; Brand, J. D.; Müllen, K.; Spiess, H. W. *Phys. Chem. Chem. Phys.* **2000**, *2*, 1735−1745.
(181) Herwig, P. T.; Enkelmann, V.; Schmelz, O.; Müllen, K. *Chem. Eur. J.* **2000**, *6*, 1834−1839.
(182) Goddard, R.; Haenel, M.; Herndon, W. C.; Krüger, C.; Zander, M. *J. Am. Chem. Soc.* **1995**, *117*, 30−41.
(183) Kübel, C.; Eckhardt, K.; Enkelmann, V.; Wegner, G.; Müllen, K. *J. Mater. Chem.* **2000**, *10*, 879−886.
(184) Dötz, F.; Brand, J. D.; Ito, S.; Gherghel, L.; Müllen, K. *J. Am. Chem. Soc.* **2000**, *122*, 7707−7717.
(185) Ghergel, L.; Brand, J. D.; Baumgarten, M.; Müllen, K. *J. Am. Chem. Soc.* **1999**, *121*, 8104−8105.
(186) van Willigen, H.; van Broekhaven, J. A. M.; de Boer, E. *Mol. Phys.* **1967**, *12*, 533.
(187) Jesse, R. E.; Biloen, P.; Prins, R.; van Voorst, J. D. W.; Hoijtink, G. J. *J. Chem. Phys. 6* **1963**, 633.
(188) Bechgaard, K.; Parker, V. D. *J. Am. Chem. Soc.* **1972**, *94*, 4749.
(189) Glasbeck, M.; van Voorst, J. D. W.; Hojitink, G. J. *J. Chem. Phys.* **1966**, *45*, 1852.
(190) Krusic, P. J.; Wasserman, E. *J. Am. Chem. Soc.* **1991**, *113*, 2322−2323.
(191) Clar, E. *Ber. Dtsch. Chem. Ges.* **1936**, *69*, 607.
(192) Klevens, H. B.; Platt, J. R. *J. Chem. Phys.* **1949**, *17*, 470.
(193) Gherghel, L.; Müllen, K. Manuscript in preparation.
(194) Boden, N.; Bushby, R. J.; Clements, J.; Movaghar, B. *J. Mater. Chem.* **1999**, *9*, 2081−2086.
(195) Marguet, S.; Markovitsi, D.; Millié; Sigal, H.; Kumar, S. *J. Phys. Chem. B* **1998**, *102*, 4697−4710.
(196) Desiraju, G. R.; Gavezzotti, A. *Acta Crystallogr.* **1989**, *B45*, 473−482.
(197) Dias, J. R. *Thermochim. Acta* **1987**, *122*, 313−337.

(198) Ferraris, G.; Jones, D. W.; Yerkess, J. *Z. Kristallogr.* **1973**, *138*, 113−128.
(199) Shibata, K.; Kulkarni, A. A.; Ho, D. M.; Pascal, R. A., Jr. *J. Am. Chem. Soc.* **1994**, *116*, 5983−5984.
(200) Shibata, K.; Kulkarni, A.; Ho, D. M.; Pascal, R. A. J. *J. Org. Chem.* **1995**, *60*, 428−434.
(201) Frampton, C. S.; MacNicol, D. D.; Rowan, S. J. *J. Mol. Struct.* **1997**, *405*, 169−178.
(202) Baird, T.; Gall, J. H.; MacNicol, D. D.; Mallinson, P. R.; Michie, C. R. *J. Chem. Soc., Chem. Commun.* **1988**, 1471−1473.
(203) Barnett, L.; Ho, D. M.; Baldridge, K. K.; Pascal, R. A. J. *J. Am. Chem. Soc.* **1999**, *121*, 727−733.
(204) Pena, D.; Pérez, D.; Guitián, E.; Castedo, L. *Org. Lett.* **1999**, *1*, 1555−1557.
(205) Robertson, J. M.; Trotter, J. *J. Chem. Soc.* **1961**, 1280−1284.
(206) Herndon, W. C. *J. Am. Chem. Soc.* **1990**, *112*, 4546−4547.
(207) Herndon, W. C.; Nowak, P. C.; Connor, D. A.; Lin, P. *J. Am. Chem. Soc.* **1992**, *114*, 41−47.
(208) Dong, W.; Baird, T.; Fryer, J. R.; Gilmore, C. J.; MacNicol, D. D.; Bricogne, G.; Smith, D. J.; O'Keefe, M. A.; Hövmoller, S. *Nature* **1992**, *355*, 605−609.
(209) Downing, G. A.; Frampton, C. S.; MacNicol, D. D.; Mallinson, P. R. *Angew. Chem., Int. Ed. Engl.* **1994**, *33*, 1587−1589; *Angew. Chem.* **1994**, *106*, 1653−1655.
(210) Hendel, W.; Khan, Z. H.; Schmidt, W. *Tetrahedron* **1986**, *42*, 1127−1134.
(211) Muetterties, E. L.; Bleeke, J. R.; Wucherer, E. J.; Albright, T. A. *Chem. Rev.* **1982**, *82*, 499−525.
(212) Rogers, R. D.; Atwood, J. L.; Albright, T. A.; Lee, W. A.; Rausch, M. D. *Organometallics* **1984**, *3*, 263−270.
(213) Lacoste, M.; Astruc, D. *J. Chem. Soc., Chem. Commun.* **1987**, 667−669.
(214) Chávez, I.; Cisternas, A.; Otero, M.; Román, E.; Müller, U. *Z. Naturforsch.* **1990**, *45b*, 658−666.
(215) Porter, L. C.; Polam, J. R.; Mahmoud, J. *Organometallics* **1994**, *13*, 2092−2096.
(216) Nagashima, H.; Suzuki, A.; Nobata, M.; Itoh, K. *J. Am. Chem. Soc.* **1996**, *118*, 687−688.
(217) Buchanan, J. W.; Reddic, J. E.; Grieves, G. A.; Duncan, M. A. *J. Phys. Chem. A* **1998**, *102*, 6390−6394.
(218) Hoffman, R. E.; Shabtai, E.; Rabinovitz, M.; Iyer, V. S.; Rai, A. K.; Bayrd, E.; Scott, L. T. *J. Chem. Soc., Perkin Trans. 2* **1998**, 1659−1664.
(219) Munakata, M.; Wu, L. P.; Kuroda-Sowa, T.; Maekawa, M.; Suenaga, Y.; Ning, G. L.; Kojima, T. *J. Am. Chem. Soc.* **1998**, *120*, 8610−8618.
(220) Barthram, A. M.; Cleary, R. L.; Kowallick, R.; Ward, M. D. *Chem. Commun.* **1998**, 2695−2696.
(221) von Ragué Schleyer, P.; Kiran, B.; Simion, D. V.; Sorensen, T. S. *J. Am. Chem. Soc.* **2000**, *122*, 510−513.
(222) Müllen, K.; Rabe, J. P. *Ann. N.Y. Acad. Sci.* **1998**, *852*, 205−218.
(223) Charra, F.; Cousty, J. *Phys. Rev. Lett.* **1998**, *80*, 1682−1685.
(224) Iyer, V. S.; Yoshimura, K.; Enkelmann, V.; Epsch, R.; Rabe, J. P.; Müllen, K. *Angew. Chem., Int. Ed. Engl.* **1998**, *37*, 2696−2699; *Angew. Chem.* **1998**, *110*, 2843−2846.
(225) Ito, S.; Herwig, P. T.; Böhme, T.; Rabe, J. P.; Rettig, W.; Müllen, K. *J. Am. Chem. Soc.* **2000**, *122*, 7698−7706.
(226) Keil, M.; Samori, P.; dos Santos, D. A.; Kugler, T.; Stafström, S.; Brand, J. D.; Müllen, K.; Bredas, J. L.; Rabe, J. P.; Salaneck, W. R. *J. Phys. Chem.* **2000**, *104*, 3967−3975.
(227) Yatabe, T.; Harbison, M.; Brand, J. D.; Wagner, M.; Müllen, K.; Samori, P.; Rabe, J. P. *J. Mater. Chem.* **2000**, *10*, 1519−1525.
(228) Müller, M.; Petersen, J.; Strohmeier, R.; Günther, C.; Karl, N.; Müllen, K. *Angew. Chem., Int. Ed. Engl.* **1996**, *35*, 886−888; *Angew. Chem.* **1996**, *108*, 947−949.
(229) Zimmermann, N. K. *Surf. Sci.* **1992**, *268*, 296.
(230) Schmitz-Hübsch, T.; Sellam, F.; Staub, R.; Törker, M.; Fritz, T.; Kübel, C.; Müllen, K.; Leo, K. *Surf. Sci.* **2000**, *445*, 358−367.
(231) Giancarlo, L. C.; Flynn, G. W. *Acc. Chem. Res.* **2000**, *33*, 491−501.
(232) Christensen, A. T.; Stromme, K. O. *Acta Crystallogr.* **1969**, *B25*, 657.
(233) Desiraju, G. R.; Parthasarathy, R. *J. Am. Chem. Soc.* **1989**, *111*, 8725.
(234) Price, S. L.; Stone, A. J.; Lucas, J.; Rowland, R. S.; Thornley, A. E. *J. Am. Chem. Soc.* **1994**, *116*, 4910.
(235) Kopitzke, J.; Wendorff, J. H. *Chem. unserer Zeit* **2000**, *34*, 4−16.
(236) Boenigk, W.; Haenel, M. W.; Zander, M. *Fuel* **1995**, *74*, 305−306.
(237) Adam, D.; Schuhmacher, P.; Simmerer, J.; Häussling, L.; Siemensmeyer, K.; Etzbach, K. H.; Ringsdorf, H.; Haarer, D. *Nature* **1994**, *371*, 141−143.
(238) Bock, H.; Helfrich, W. *Liq. Cryst.* **1995**, *18*, 387−399.
(239) Uznanski, P.; Marguet, S.; Markovitsi, D.; Schumacher, P.; Ringsdorf, H. *Mol. Cryst. Liq. Cryst.* **1997**, *293*, 123−133.
(240) Eichhorn, H. *J. Porphyrins Phthalocyanines* **2000**, *4*, 88−102.
(241) van de Craats, A. M.; Warman, J. M.; Fechtenkötter, A.; Brand, J. D.; Harbison, M. A.; Müllen, K. *Adv. Mater.* **1999**, *11*, 1469−1472.
(242) Chandrasekhar, S.; Prasad, S. K. *Contemp. Phys.* **1999**, *40*, 237−245.
(243) Boden, N.; Bushby, R. J.; Clements, J.; Movaghar, B.; Donovan, K. J.; Kreouzis, T. *Phys. Rev. B* **1995**, *52*, 13247−13280.
(244) van de Craats, A. M.; Siebbeles, L. D. A.; Bleyl, I.; Haarer, D.; Berlin, Y. A.; Zharikov, A. A.; Warman, J. M. *J. Phys. Chem. B* **1998**, *102*, 9625−9634.
(245) van de Craats, A. M.; Warman, J. M.; Müllen, K.; Geerts, Y.; Brand, J. D. *Adv. Mater.* **1998**, *10*, 36−38.
(246) van de Craats, A. M.; de Haas, M. P.; Warman, J. M. *Synth. Met.* **1997**, *86*, 2125−2126.
(247) van de Craats, A. M.; Warman, J. M.; Schlichting, P.; Rohr, U.; Geerts, Y.; Müllen, K. *Synth. Met.* **1999**, *102*, 1550−1551.
(248) van de Craats, A. M.; Warman, J. M.; de Haas, M. P.; Adam, D.; Simmerer, J.; Haarer, D.; Schuhmacher, P. *Adv. Mater.* **1996**, *8*, 823−826.
(249) Glüsen, B.; Heitz, W.; Kettner, A.; Wendorff, J. B. *Liq. Cryst.* **1996**, *20*, 627−633.
(250) Simmerer, J.; Glüsen, B.; Paulus, W.; Kettner, A.; Schuhmacher, P.; Adam, D.; Etzbach, K. H.; Siemensmeyer, K.; Wendorff, J. H.; Ringsdorf, H.; Haarer, D. *Adv. Mater.* **1996**, *8*, 815−819.
(251) Kranig, W.; Boeffel, C.; Spiess, H. W. *Macromolecules* **1990**, *23*, 3.
(252) Zamir, S.; Poupko, R.; Luz, Z.; Huser, B.; Boeffel, C.; Zimmermann, H. *J. Am. Chem. Soc.* **1994**, *116*, 1973−1980.
(253) Heiney, P. A.; Fontes, E.; De Jeu, W. H.; Riera, A.; Carroll, P.; Smith, A. B., III *J. Phys. Fr.* **1989**, *50*, 461−483.
(254) Vaes, A.; Van der Auweraer, M.; De Schryver, F. C.; Laguitton, B.; Jonas, A.; Henderson, P.; Ringsdorf, H. *Langmuir* **1998**, *14*, 5250−5254.
(255) Vaes, A.; Catry, C.; Van der Auweraer, M.; De Schryver, F. C.; Sudiwala, R. V.; Wilson, E. G.; Karthaus, O.; Ringsdorf, H. *J. Appl. Phys.* **1998**, *84*, 339−349.
(256) Tsukruk, V. V.; Bengs, H.; Ringsdorf, H. *Langmuir* **1996**, *12*, 754−757.
(257) Ogawa, K.; Yonehara, H.; Pac, C.; Maekawa, E. *B. Chem. Soc. Jpn.* **1993**, *66*, 1378−1385.
(258) Karthaus, O.; Ringsdorf, H.; Urban, C. *Makromol. Chem.-Macro. Symp.* **1991**, *46*, 347−352.
(259) Vandevyer, M.; Albouy, P. A.; Mingotaud, C.; Perez, J.; Barraud, A.; Karthaus, O.; Ringsdorf, H. *Mol. Cryst. Liq. Cryst. A* **1993**, *234*, 333−339.
(260) Schonherr, H.; Kremer, F. J. B.; Kumar, S.; Rego, J. A.; Wolf, H.; Ringsdorf, H.; Jaschke, M.; Butt, H. J.; Bamburg, E. *J. Am. Chem. Soc.* **1996**, *118*, 13051−13057.
(261) Owens, R.; Smith, D. A. *Mol. Cryst. Liq. Cryst. A* **1999**, *329*, 995−1003.
(262) Allison, H.; Boden, N.; Bushby, R. J.; Evans, S. D.; Martin, P. S. *Mol. Cryst. Liq. Cryst. A* **1997**, *303*, 273−278.
(263) Boden, N.; Bushby, R. J.; Martin, P. S.; Evans, S. D.; Owens, R. W.; Smith, D. A. *Langmuir* **1999**, *15*, 3790−3797.
(264) Antonietti, M.; Kaul, A.; Thünemann, A. *Langmuir* **1995**, *11*, 2633−2638.
(265) Antonietti, M.; Henke, S.; Thünemann, A. *Adv. Mater.* **1996**, *8*, 41.
(266) Thünemann, A. F.; Ruppelt, D.; Ito, S.; Müllen, K. *J. Mater. Chem.* **1999**, *9*, 1055−1057.
(267) Thünemann, A. F.; Ruppelt, D.; Burger, C.; Müllen, K. *J. Mater. Chem.* **2000**, *10*, 1325−1329.
(268) Brand, J. D.; Kübel, C.; Ito, S.; Müllen, K. *Chem. Mater.* **2000**, *12*, 1638−1647.
(269) Janietz, D.; Festag, R.; Schmidt, C.; Wendorff, J. H. *Liq. Cryst.* **1996**, *20*, 459−467.
(270) Maliszewskyj, N. C.; Mindyuk, O. Y.; Heiney, P. A.; Josefowicz, J. Y.; Schuhmacher, P.; Ringsdorf, H. *Liq. Cryst.* **1999**, *26*, 31−36.
(271) Reitzel, N.; Hassenkamp, T.; Balashev, K.; Jensen, T. R.; Howes, P. B.; Kjaer, K.; Fechtenkötter, A.; Ito, S.; Müllen, K.; Bjornholm, T. *Chem. Eur. J.* **2001**, accepted.
(272) Uckert, F.; Tak, Y.-H.; Müllen, K.; Bässler, H. *Adv. Mater.* **2000**, *12*, 905−908.
(273) Randic, M.; Guo, X. *New J. Chem.* **1999**, 251−260.
(274) Watson, M. D.; Müllen, K. Manuscript in preparation.
(275) Teraguchi, M.; Masuda, T.; Fechtenkötter, A.; Müllen, K. *Polym. Bull.* **2000**, *44*, 255−260.
(276) Keegstra, M. A.; De Feyter, S.; De Schryver, F. C.; Müllen, K. *Angew. Chem., Int. Ed. Engl.* **1996**, *35*, 774−776; *Angew. Chem.* **1996**, *108*, 830−833.
(277) Wiesler, U.-M.; Berresheim, A.; Morgenroth, F.; Lieser, G.; Müllen, K. *Macromolecules* **2001**, *34*, 187−199.
(278) Berresheim, A. J. Ph.D. Thesis, University of Mainz, 2000.
(279) Hart, H. *Pure Appl. Chem.* **1993**, *65*, 27.
(280) Weil, T.; Herrmann, A.; Müllen, K. Manuscript in preparation.

(281) Karni, Y.; Jordens, S.; de Belder, G.; Hofkens, H.; Schweitzer, G.; De Schryver, F.; Herrmann, A.; Müllen, K. *J. Phys. Chem. B* **1999**, *103*, 9378−9381.

(282) Hofkens, J.; Vosch, T.; Maus, M.; Köhn, F.; Cotlet, M.; Weil, T.; Herrmann, A.; Müllen, K.; De Schryver, F. C. *Chem. Phys. Lett.* **2001**, *333*, 255−263.

(283) De Feyter, S.; Gesquiere, A.; Abdel-Mottaleb, M. M.; Grim, K.; De Schryver, F.; Meiners, C.; Valiyaveetil, S.; Müllen, K. *Acc. Chem. Res.*, submitted for publication.

(284) Böhme, T.; Simpson, C.; Müllen, K.; Rabe, J. Manuscript in preparation.

(285) Giancarlo, L. C.; Flynn, G. W. *Annu. Rev. Phys. Chem.* **1998**, *49*.

CR990322P